RSC Advances

ROYAL SOCIETY OF CHEMISTRY

www.rsc.org/advances

Tailoring PES Nanofiltration Membranes through Systematic Investigations on the Effect of Prominent Design, Fabrication and Operational Parameters

Mohammad Amin Alaei Shahmirzadi[a], Seyed Saeid Hosseini[a*], Guoling Ruan[b], N. R. Tan[c]

[a] Department of Chemical Engineering, Tarbiat Modares University

Tehran, 14115-114, Iran

[b] Institute of Seawater Desalination and Multipurpose Utilization,

Tianjin, 300192, China

[c] Research & Development Dept., HOSSTECH Group,

Singapore, 528844, Singapore

* saeid.hosseini@modares.ac.ir

Abstract:

Design and Fabrication of nanofiltration membranes with desired characteristics and separation performance is of paramount importance. In this study various asymmetric nanofiltration membranes are designed and fabricated using polyethersulfone (PES) via phase inversion technique. The effects of variation in polymer concentration, solvent type, additives in dope solution and composition of coagulating agent are studied as selected design parameters. On the other hand, the effects of variation in solvent evaporation time, coagulation bath temperature, casting speed (shear rate) and membrane thickness are investigated as selected fabrication parameters. The findings reveal that increasing polymer concentration, promoting delayed demixing through change of solvent and composition of coagulating agent as well as decreasing coagulation bath temperature, increasing solvent evaporation time and membrane thickness result in NF membranes with less overall porosity and mean pore size, lower water flux and higher salt rejection. Moreover, addition of hydrophilic organic acids (i.e., ascorbic and citric acids) in dope solution and increment of casting shear rate promote membrane overall porosity, water flux and, salt rejection. Membranes derived from PES/NMP (30/70 wt. %) can offer maximum rejection of 47.35% and 99.84% for NaCl and $MgSO_4$, respectively. The pure water flux in the membranes can be enhanced up to 54.88 lit.m^{-2}.h^{-1} through addition of 1 wt. % citric acid into dope solution. In terms of operational parameters, increase in both feed pressure and pH can enhance the membrane flux and salt rejection. The findings in this study provide useful guidelines and recipes for design and fabrication of high performance asymmetric NF membranes with desired microstructure, productivity and separation performance.

Keyword: Nanofiltration membranes, Design and fabrication parameters, Polyethersulfone, Phase inversion, Separation performance

1. Introduction

Membrane technology has gained widespread acceptance for variety of separation applications ranging from microfiltration to gas separation, pervaporation and fuel cells [1-5]. Many activities are in progress in various parts of the world on material synthesis, membrane fabrication, membrane modification, process design and development, process modeling and optimization, all aiming to overcome the remaining obstacles and to improve the competitiveness of the membrane technologies [6-12]. Nanofiltration (NF) is relatively a new type of pressure-driven membrane technology that lies between ultrafiltration (UF) and reverse osmosis (RO) [13]. NF membranes are employed effectively for separation of charged and/or uncharged species in the size range of about 1-10 nm. The governing mechanisms in NF membranes are solution diffusion, Donnan effect, dielectric exclusion, electromigration or a combination of them [14]. Numerous advantages such as energy efficiency, high flux as well as higher rejection of multivalent than monovalent ions [14, 15] have led to the widespread application of NF membranes in various industries including but not limited to water softening [16, 17], seawater desalination [18, 19], brackish water treatment [20-22], dye removal [23-25], industrial wastewater treatment and reuse [26-28], food and beverage processing [29] and pharmaceutical industry [30].

Development of high performance NF membranes require thorough understanding about proper materials selection, formulation, design and fabrication procedures in addition to the adoption of appropriate knowhow and skills. Phase inversion can be described as a process of making membranes in which an initially homogeneous polymer solution is transformed into a solid structure through a complicated while controlled procedure. Non-solvent induced phase separation (NIPS), thermal-induced phase separation (TIPS), Evaporation-induced phase separation (EIPS) and Vapor-induced phase separation (VIPS) are among the wellestablished phase inversion processes. NIPS is commonly used for fabrication for asymmetric NF membranes. According to this procedure, a polymer solution is cast on a proper support, then immersed in a coagulation bath containing a non-solvent or a blend of non-solvents [31]. The non-solvent diffuses into the polymer solution and the solvent escapes from polymeric solution to the non-solvent bath known as demixing process through which a system comprised of a polymer-rich and polymer-lean phases is formed. The former results in the formation of a membrane solid matrix, while the latter creates membrane pores [32].

Essentially, various kinetic and thermodynamic parameters including selection of polymer, solvent, non-solvent and additive to the polymer solution and its composition play important roles in the properties and characteristics of the ultimate membranes [33].

These parameters may generally be classified into two main groups of design and fabrication as shown in Fig. 1. Design parameters may include material selection, polymer concentration in the dope, solvent type, additives in the dope solution, and composition of coagulating agent. Various materials including but not limited to polysulfone [34], cellulose acetate[35], polyvinylidene fluoride [36] have been used for preparation of asymmetric NF membranes. Among them, polyethersulfone (PES) has been widely used for preparation of variety of membranes mainly due to its particular characteristics such as prominent oxidative, thermal ($T_g{\sim}220^{\circ}C$) hydrolytic, chemical and mechanical stability [37, 38]. On the other hand, it is shown that the polymer concentration can play a major role in the structure of the membrane. Study by Balta et al [39] revealed that increase in the polymer concentration led to the formation of NF membranes with less porosity and less finger-like pores and consequently decreased water flux and increased salt rejection. Membranes with different morphology and performance can be achieved depending on the type and nature of solvents and non-solvent.

Various approaches such as bulk modification, blending, additive embedding, surface coating, interfacial polymerization, grafting (e.g., photon-induced, Gamma ray, electron/ion beam-induced, plasma-induced, thermal-induced), plasma treatment, immobilization and surface-initiated ATRP have been applied for altering the hydrophobic nature of PES-derived membranes [40]. The use of additives consisting of functional groups has also been considered as the possible techniques for altering the hydrophilicity, surface roughness, surface charge and the pore size of the membranes [41-43]. For instance, pore-forming agents, such as polyvinylpyrrolidone (PVP) and polyethylene glycol (PEG) have been added to the polymer solution for improving the permeability of the membranes [44]. Another effective parameter is composition of coagulating agent. While water has been the dominating coagulation bath, several types of additive such as ethanol [45, 46], isopropanol [45-47], 2-Butanol [48] and NMP [49] have been examined separately or as additives to water in order to tailor the characteristics of the coagulating agent.

Apart from the design parameters, fabrication parameters also play important role in the properties of the resultant membranes. For example, the influence of solvent evaporation time was investigated in some previous works [50, 51]. It is also shown that increasing coagulation bath temperature results in accelerated phase inversion rate and consequently improved water flux [52-54]. However, in some cases, decreasing of water flux has been reported [45]. The casting speed also affects the membrane morphology, porosity and pore size by which is attributed to the alternation of molecular orientation caused by induced shear rate [34, 55-57]. It is also shown that the overall thicknesses of the membrane as well as the top layer increase by increasing the casting knife gap [58-60].

The main objective of the present research study is to perform a systematic investigation on the effect of key parameters in development of asymmetric NF membranes from the viewpoint of formation, structural characteristics, productivity and separation performance. For this purpose, the effect of various design parameters such as polymer concentration in the dope, solvent type, additives in dope solution, composition of coagulating agent as well as various fabrication parameters such as solvent evaporation time, coagulation bath temperature, casting speed (casting shear rate) and membrane thickness on the characteristics and performance of the membranes are investigated and analyzed. Besides, the effect of feed pressure and pH as operational parameters are studied in details. To our best knowledge, and based on the detailed review and analysis of the prior works, this is the first comprehensive report on systematic investigation of NF membranes. Furthermore, the effects of addition of selected hydrophilic additives (i.e., ascorbic and citric acids) into dope solution are assessed for the first time in the case of PES NF membranes.

2. Experimental

2.1. Materials

Polyethersulfone (PES, Ultrason E6020P, MW = 58,000 g/Mol) was supplied by BASF (Germany). N-Methyl-2-pyrrolidone (NMP) and N, N-Dimethylacetamide (DMAc) both from Merck (Germany) were used as solvent for preparation of dope solutions mainly because of good miscibility with PES. Ascorbic acid ($C_6H_8O_6$, $pKa = 4.10$) and citric acid ($C_6H_8O_7$, $pKa = 3.15$) both from Merck (Germany) were employed as additives to the dope solutions. NaCl and $MgSO_4$ salts were obtained from Merck Ind. Ethanol and distilled water were employed as coagulating agents. The chemical structure of the materials used in this study are illustrated in Fig. 2.

2.2. Membrane Preparation

Dope solutions were prepared by dissolving prescribed amounts of PES flakes in the respective solvents. Ascorbic and citric acids were added in the prescribed amounts to the selected dope solutions as additives. The solutions were stirred for at least 24 hrs at 300 rpm and at room temperature to ensure complete dissolution. After formation of a homogeneous solution, dope solutions were held at the ambient temperature about 24 hrs and degassed. Then the solutions were cast onto a glass plate using a semi-automatic film applicator with adjustable gap at controlled temperature and relative air humidity. The nascent films on the glass plate were immersed immediately in the coagulation bath (except of one case in order to investigate the effects of solvent evaporation time) and remained for 24 hrs to allow residual solvents to leach out. Finally, the membranes were kept between two filter papers at room temperature and dried. The reference conditions for membrane formation are provided in Table 1. The effect of various design parameters including polymer concentration in the dope, solvent type, additive type and amount in dope solution, composition of coagulating agent as well as fabrication parameters such as solvent evaporation time, coagulation bath temperature, casting speed (casting shear rate) and membrane thickness on the characteristics and performance of the membranes were studied systematically.

2.3. Membrane Characterizations

2.3.1. Morphology analysis

A VEGA (TESCAN, Czech Republic) scanning electron microscope (SEM) was used for characterization of cross-sectional morphology of the fabricated membranes. The membrane samples were fractured in liquid nitrogen and sputtered with gold. ImageJ software (version 1.48) was employed for further analysis of the types and population of macrovoids in the cross-section of membranes.

2.3.2. Porosity and pore size measurements

Overall porosity (ε) was calculated as a function of the membrane weight using the following equation [61]:

$$\varepsilon = \frac{w_1 - w_2}{Al\rho} \tag{1}$$

Where w_1 and w_2 are the weights (kg) of the wet and dry membranes; A is the membrane effective area (m^2), ρ is the density of water (998 $kg.m^{-3}$) and l is the membrane thickness (m). Guerout–Elford–Ferry equation (Eq. (2)) was employed to determine membrane mean pore radius (r_m) on the basis of pure water flux and porosity data [62]:

$$r_m = \sqrt{\frac{(2.9 - 1.75\varepsilon) \times 8\mu l Q}{\epsilon A \Delta P}} \tag{2}$$

Where μ is the viscosity of water (8.9×10^{-4} Pa.s), Q is the volumetric flow rate of permeate pure water ($m^3.s^{-1}$) and ΔP is the operating pressure (Pa). Average pore size, r_m, was determined by filtration velocity method, in which pure water flux of the wet membrane was measured by applying pressure (10 bar) for a limited period.

2.3.3. Contact angle measurements

To evaluate membrane surface properties, contact angles were measured using the sessile drop method with a goniometer (G10, KRUSS, Germany). Deionized water was used as the probe liquid in all the measurements. To minimize the experimental error, the contact angle was measured at five random locations for each sample at room temperature, and then the average value was reported.

2.4. Performance evaluation

The performance of the membranes were evaluated using a bench scale set-up as shown in Fig. 3. Rectangular shaped membrane sheets with effective surface area of 15 cm^2 were cut and sandwiched between the testing cells. The feed was pumped into the cell by using a high pressure pump, flowing tangentially to the membrane surface. The permeate stream was directed to the permeate tank while the retentate stream returned to the feed tank. In this way, the concentration of the feed remains almost unchanged due to limited amount of permeate stream. The feed flow rate and stream pressures were adjusted using back pressure regulator and bypass valves. The following procedure was used in all experiments:

1) Before starting the experiments, each membrane was soaked in deionized water for 2 hrs to provide required saturation and wetting in the membrane structure.
2) Each membrane sheet was firstly subjected to pre-compaction at 15 bar for 2 hrs using pure water. However, pure water permeate flux was measured at 10 bar and feed flow rate of 5 lit.min^{-1} using Eq.(3)

$$J = \frac{V}{A.\Delta t} \tag{3}$$

Where V is the volume of permeated water (lit), A is the membrane area (m^2) and Δt is the permeation time (hr).

3) The single salt rejection of the membranes was measured using a synthetically designed salt (formulated based on a typical seawater properties) containing 10,500 ppm of NaCl solution and 1,300 ppm of $MgSO_4$ solution.
4) The feed solution was circulated for about 1 hr until the system became steady state, and then the permeate flux was measured at 10 bar and feed flow rate=5 lit.min^{-1}. Samples from feed and permeate was collected and analyzed separately using a standard conductivity meter (MIC 99702, Taiwan).
5) The single salt rejection (R) was measured using the Eq. (4).

$$R(\%) = \left(1 - \frac{C_P}{C_f}\right) \times 100\% \tag{4}$$

3. Results and discussion

3.1. Effect of polymer concentration in dope solution on the structure and performance of NF membranes

The effect of polymer concentration in the dope solution on the water flux and salts rejection of the NF membranes prepared using NMP and DMAc as solvents is shown in Fig. 4. It can be seen that polymer concentration has considerable effect on the membrane permeation and separation performance. According to Fig. 4 (a), the pure water flux decreased from 38.35 $lit.m^{-2}.hr^{-1}$ to 2.78 $lit.m^{-2}.hr^{-1}$ for the membranes prepared using 24 and 30 wt. % PES in DMAc, respectively. Similarly, the pure water flux decreased from 27.65 $lit.m^{-2}.hr^{-1}$ to 1.24 $lit.m^{-2}.hr^{-1}$ for the membranes prepared using 24 and 30 wt. % PES in NMP, respectively. This can be attributed to the fact that increase in the PES concentration results in the increment in the dope viscosity. This increase in viscosity consequently brings about reduction of solvent and non-solvent exchange rate and thus polymer concentration increases at the interphase of dope solution and coagulating agent. Thus, less amounts coagulants can penetrate to the dope solution and precipitation rate decreases through delayed demixing. It is well demonstrated that the instantaneous demixing leads to a finger-like structure, while delayed demixing leads to a sponge-like structure [63]. Fig. 5 presents SEM cross-section images of membranes prepared using dopes with different polymer concentrations. It can clearly be seen that, regardless of the solvent type, membranes formed from low polymer concentration (i.e., 24 wt. %) comprised of finger-like macrovoids with interconnection extended to the bottom of the membranes. However, increasing polymer concentration suppressed formation of finger-like macrovoids and created more spongy-like porous structures. Thus, it can be prescribed that increase in polymer concentrations and delayed demixing result in membranes with lesser porosity, less finger-like pores, lower mean pore size, while denser and thicker upper layer upon. Data in Table 1 provide a good overview on the trend of changes in the morphological and structural characteristics of membranes as a result of change in polymer concentration. Data reveal that increase in the polymer concentration led to the formation of up to about 11% thicker NF membranes. Similar results are reported elsewhere [45]. This may arise from the fact that higher polymer concentration provides less opportunity for the penetration of coagulation agent and accordingly less contraction ratio is provided due to the slowed demixing rate.

On the other hand, by increase in polymer concentration, the mean pore size decreased from 4.93 nm to 1.20 nm and from 4.96 to 1.64 in NF membranes prepared using NMP and DMAc, respectively. Similarly, the porosity decreased by about 17% and 19% in NF membranes prepared from NMP and DMAc, respectively. Higher porosity can be attributed to higher diffusional exchange between solvent and coagulant at lower polymer concentration [45]. According to the data in Table 1 and also as shown in Fig. 5, increase in the polymer concentration brought about reduction in the area fraction of macrovoids in the cross section of membranes, reduced number of macrovoids and turned the overall membranes morphology into a more spongy-like structure. In addition, the contact angle of prepared membrane increases from 63.4^o to 75.5^o and from 60.5^o to 72.9^o in NF membranes prepared from dopes containing 24 and 30 wt. % polymer in NMP and DMAc, respectively. Sotto et al. [61] determined that increasing polymer concentration decreases the solvent and coagulant diffusional exchange rate and hence, the surface porosity and pore size decreases. It should be noted that the wettability of the membrane is influenced by the membrane material as well as the surface porosity and roughness. Thus, since the materials are the same, the greater contact angle of the membrane prepared from the dope with higher concentration can mainly be attributed to the decreased surface porosity [64]. In other words, higher polymer concentration leads to lower surface porosity causing decrement in the hydrophilicity of the membranes and water flux.

The effect of polymer concentration in the dope solutions on the performance of NF membranes was investigated in terms of monovalent and divalent salt rejections. Generally, increase in polymer concentration led to improvements in both NaCl and $MgSO_4$ rejection of membranes. According to Fig. 4 (b), NaCl rejection increased from 23.36% to 47.35% and from 18.62% to 40.80% in NF membranes prepared from dope containing 24 and 30 wt. % polymer in NMP and DMAc, respectively. Membranes offered even higher rejections for $MgSO_4$. According to Fig. 4 (c), $MgSO_4$ rejection increased from 86.35% to 99.84% and 82.78% to 99.10% in NF membranes prepared from dope containing 24 and 30 wt. % polymer in NMP and DMAc, respectively. Due to negative surface charge of polyethersulfone membranes, the separation mechanism of these membrane is not only affected by steric hindrance, but also by charge effect interaction. According to Donnan effect, if a negatively charged salt ion is rejected because of electrostatic charge repulsion with negative surface charge of PES membrane, then the counter ion will also have to be rejected to neutralize electric charge across the membrane. For salts, an increase in co-ion charge and a decrease in counter ion charge improve salts rejection [65]. Because of higher charge of sulfate ions, the rejection of Mg^{2+} ions also increases due to Donnan effect. On the other hand, as reported by Ali et al. [57], the surface charge density of the membrane increases by decrement of membrane pore size. As exhibited in Table 1, membranes prepared from high polymer concentrations possessed smaller pores and high surface charge density. Consequently, smaller pore size increases salts rejection through both physical size sieving and electrostatic repulsion mechanisms.

3.2. The effect of solvent type on the structure and performance of NF membranes

Several studies have demonstrated the important role of solvent selection on the membrane properties and performance. This was investigated in the present study and the effect of solvent type on pure water flux and salts rejection are exhibited in Fig. 4. According to Fig. 4 (a), membranes prepared using DMAc as the solvent exhibited higher water flux than those prepared using NMP. This trend was regardless of the polymer concentration in the dope solution; noting that the difference between the pure water flux of the membranes prepared by the two solvents was minimal when the polymer concentration in the dope was 30 wt. %. The pure water flux in NF membranes prepared from dopes solutions containing 24 and 30 wt. % PES in DMAc was 38.35 lit.m^{-2}.hr^{-1} and 2.78 lit.m^{-2}.hr^{-1}, respectively. However, the pure water flux in NF membranes prepared from dopes solutions containing 24 and 30 wt. % PES in NMP was 27.65 lit.m^{-2}.hr^{-1} and 1.24 lit.m^{-2}.hr^{-1}, respectively. Therefore, the membrane prepared using DMAc exhibited higher pure water flux compared to those prepared using NMP. According to Table 1, this result can be attributed to higher porosity, lower thickness and hydrophilic nature of the membrane prepared using DMAc. As porosity and hydrophilicity increases and membrane thickness decreases and the water permeation through the membrane increases.

Analysis of the morphology of the membranes can provide useful insights about the effect of solvent type on the properties of the membranes. According to cross sectional SEM images shown in Fig. 5, switching solvent from DMAc to NMP enabled suppression in number and progress of macrovoids to some extent. Instead, relatively large macrovoids were formed.

The following points can provide more and useful insights for explanation of the effect of solvent type on the morphology and performance of NF membranes:

1) The solubility parameter and mutual diffusivity between solvent and non-solvent in coagulation bath is an important factor in membrane preparation [66]. Smaller difference between the solubility parameters results in faster/instantaneous demixing causing formation of porous top layer and finger-like pores in the support layer. On the other hand, delay demixing is often related to the formation of a dense layer. The

solubility parameter data of various components are shown in Table 2, indicating that the difference in solubility parameter between DMAc and water is the highest and this attributed to the fact that the porosity, number of finger-like pore and mean pore size of membranes prepared from this solvent is increased. In addition, the diffusivity coefficient of intended solvent and coagulant systems was calculated using Wilke-Chang equation and shown in Table 3. According to Eq. 5, the diffusivity of solute *a* into solvent *b* ($D_{a\text{-}b}$ ($cm^2.s^{-1}$)) can be described by:

$$D_{a-b} = 7.4 \times 10^{-11} \frac{(\varphi_b M_b)^{0.5}.T}{\eta_b.{V_a}^{0.6}} \quad (5)$$

Where φ, μ, V_A, M_b and T are the association factor, viscosity ($gr.cm^{-1}.s^{-1}$), molar volume at boiling point ($cm^3.kmol^{-1}$), molecular weight of the solvent ($gr.kmol^{-1}$), and temperature (K), respectively. The average mutual diffusivities of DMAc-water system is higher than NMP-water system. By increasing diffusion rate between solvent and non-solvent, the instantaneous demixing is occurred which led to increment in porosity in top and support layer [66]. A strong interaction among solvent and non-solvent is related to a small difference between solubility parameters of solvent and non-solvent. Lower mutual diffusivity and less porosity are the results of strong interaction among solvent and non-solvent [67].

2) Another aspect is consideration of delay time (time from immersion of a polymer film into a coagulant bath to the inception of liquid–liquid demixing) and gelation time (time between demixing and solidification) and their role in the phase diagram (Fig. 6 (a)) [68]. A finger-like structure with very thin skin layer is generally expected for instantaneous demixing process, whereas a sponge-like structure with thick skin layer is usually observed for delayed demixing process [66]. According to the three phase diagram for water/DMAc/PES and water/NMP/PES systems (Fig. 6 (b)), the theoretical and

experimental binodal curve of water/DMAc/PES system is closer to the polymer–solvent axis compared to that of water/NMP/PES system. Therefore less water is needed for the precipitation of PES (unstability of polymer film) in water/DMAc/PES system [69]. The time to first precipitation may be almost instantaneous for water/DMAc/PES system. The final structure of membrane depends on domination of delayed or instantaneous demixing. According to Fig. 6 (b), instantaneous demixing occurred for water/DMAc/PES compared to that of water/NMP/PES system that led to formation of thin skin layer and finger-like pores in support layer [64].

3) As reported by Hasbullah et al. [70], boiling points of solvent contribute positively to dope solution viscosity. Accordingly, higher boiling point of NMP (202 ^{o}C) than that of DMAc (166 ^{o}C) results in dope solutions with increased viscosity. As mentioned above, this increase in viscosity resulting in reduction of solvent and non-solvent exchange rate and delayed demixing occurred. Consequently, a membrane with lower porosity, less finger-like pore, lower mean pore size is formed.

Data in Table 1 provide a good overview on the trend of changes in the morphological and structural characteristics of membranes as a result solvent selection. For example, data reveal that membranes prepared using DMAc as solvent experienced more contraction and possessed lower thickness compared to their counterparts prepared using NMP. In addition, the mean pore size of the membranes prepared using DMAc was relatively high especially when higher dope concentrations were used. This is well in agreement with the pure water flux in the membranes. The exchange rate between solvent and coagulant will affect the pore size. It should be noted that the diffusional exchange rate between solvent and coagulant in DMAc/water system is faster than NMP/water system and because of delayed demixing, the solvent outflow is faster than the coagulant inflow. In this case, the pores tend to collapse and shrink [71]. On the other hand, the porosity of prepared membrane decrease from 55.5% to 46.2% and from 58.9% to 47.6% in NF membranes prepared from dope containing 24 and 30 wt. % polymer in NMP and DMAc, respectively. In fact, when DMAc was used as solvent, the instantaneous demixing occurred which led to formation of more porous structure as also reported previously by others [66]. As shown in Table 1, when NMP was used as solvent, the solvent and coagulant diffusional exchange rate decreased and hence, the surface porosity and pore size decreased. The greater contact angle of NMP-based membranes in comparison with DMAc-based membranes can be attributed to the decreased surface porosity [61]. Thus, DMAc-based membranes exhibited higher pure water flux. This improvement in pure water flux can be attributed to increase of membrane hydrophilicity.

Considering the effect of solvent type on the membrane performance, according to Fig. 4 (b), NaCl rejection increased from 23.36% to 47.35% and from 18.62% to 40.80% in NF membranes prepared from dope containing 24 and 30 wt. % polymer in NMP and DMAc, respectively. According to Fig. 4 (c), $MgSO_4$ rejection increased from 86.35% to 99.84% and 82.78% to 99.10% in NF membranes prepared from dope containing 24 and 30 wt. % polymer in NMP and DMAc, respectively. The rejection of both monovalent and divalent salts were higher in NMP-based membranes in comparison to DMAc-based membranes which can be related to smaller pore size in NMP-based membrane which increases salts rejection through both physical size sieving and electrostatic repulsion mechanisms.

3.3. The effect of additive type and concentration in dope solution on the properties and performance of NF membranes

The effect of addition of ascorbic acid as a polyhydroxy acid and citric acid as a poly acid and their concentration on the characteristics and performance of NF membranes were investigated. This was based on the idea that the incorporation of these acids may enhance performance of membranes through altering surface and structural characteristics. Investigation was carried out on the NF membranes prepared at reference conditions using dope containing 24 wt. % PES dissolved in DMAc. According to Fig. 7 (a), addition of both acids resulted in enhanced pure water flux in the membranes. The pure water flux of PES membranes increased from 38.35 lit.m^{-2}.h^{-1} (bare) to 52.99 lit.m^{-2}.h^{-1} and 54.88 lit.m^{-2}.h^{-1} by addition of 1 wt. % ascorbic and citric acids, respectively. However, further addition beyond 1 wt. % had negative effects. Pure water flux of modified membrane is expected to be higher than bare membranes. As shown in Table 4, improvement of water flux can be attributed to membrane thickness, porosity and hydrophilicity. Structural analysis and characterization of membranes can provide useful information about the performance of the membranes. The porosity of the membranes increased to 75.87% and 77.68% upon addition of ascorbic and citric acids up to 1.0 wt. %, respectively. This can be attributed to the interactions between additive with the component of casting solution (polymer and solvent). By addition of both organic acid in the dope solution, hydrogen bonds are formed between hydrogen atoms of organic acids and the oxygen atoms of polyethersulfone; accordingly, weaker interactions occur between polymer chains. In addition, the hydrophilic nature of organic acids and formation of hydrogen bonds between additive molecules and DMAc, decreases the ratio of the solvent out-diffusion to the coagulant (water) inter-diffusion which causes to instantaneous demixing [72, 73]. Instantaneous demixing results in formation of macrovoid, porous top and support layers and lower concentration of the polymer at the surface which lead to thinner skin layer [66]. However, further addition of organic acids beyond 1 wt. % results in the increase in binding force between polymer chains and additive molecules and accordingly the remaining free volume is reduced due to the tighter and stronger entanglements. Moreover, according to the data in Table 4, and in comparison to the reference membranes thickness (100 µm), thinner membranes were obtained from the dopes containing either ascorbic or citric acids (91 µm and 89 µm for $A_{1.5}$ and $C_{1.5}$ respectively). The addition of additives decreases the ratio of the solvent out-diffusion to the coagulant (water) inter-diffusion and provides more opportunity for the penetration of coagulation agent and accordingly more contraction ratio is provided due to the faster demixing [72]. It was also found that the addition of both acids improved the hydrophilic properties of the membranes largely attributed to the hydrophilic functional groups of organic acids [72]. The effect of ascorbic acid on the contact angle of the membranes was more than that of citric acid. The contact angle reduced from 60.5^{o} to 38.6^{o} and 45.3^{o} upon addition of 1.5 wt. % ascorbic and citric acids, respectively.

Also, according to Fig. 7 (b) and (c), the rejection of both monovalent and divalent salts increased by increasing the concentration of both organic acids in the dope solutions. The salts rejection increases from 18.62% (bare) to 28.54% ($A_{1.5}$) and 30.14% ($C_{1.5}$) for NaCl and from 82.78% (bare) to 88.21% ($A_{1.5}$) and 90.78% ($C_{1.5}$) for $MgSO_4$, respectively. Size exclusion (steric hindrance) and electrostatic charge repulsion are two important mechanisms that may have affected the rejection of ionic solutes. It is shown that PES membranes have negative charge due to breakdown of surface functional groups or adsorption of ions from the aqueous solution [74]. As reported in Table 4, mean pore size of modified membrane is smaller than unmodified membrane. Increment in salt rejection by addition of organic acid might be attributed to two factors: (i) reduction of pore size of the membrane which increasing the salt rejection through size exclusion mechanism and (ii) increment in surface negative charge by addition of organic acid and lower pore size (higher surface charge density) which increasing the salt rejection through electrostatic charge repulsion [72].

3.4. The effect of type and concentration of coagulating agent on the properties and performance of NF membranes

The effects of adding methanol to the coagulation bath (distilled water) were investigated for the NF membranes prepared at reference conditions using dope containing 24 wt. % PES dissolved in DMAc. In order to study the effects of composition of coagulating agent on structure and performance of PES membrane, three different compositions were employed as the coagulation bath (Table 5). The characteristics and performance of prepared membrane at different composition of coagulation agents are tabulated in Table 5. The pure water flux for different prepared membranes are depicted in Table 5. The pure water flux of membranes is reduced from 38.35 lit.m^{-2}.h^{-1} to 29.15 lit.m^{-2}.h^{-1} when methanol is added to the coagulation bath from 0 to 50 V. %. This is due to the formation of membranes with lower porosity, smaller pore size and lesser hydrophilicity and higher thickness. The pure water flux is in a good agreement with membrane structural properties. By employing a mixture of methanol and water as coagulation agent, the porosity of prepared membrane decreased from 58.9% to 52.74% and mean pore size decreased from 4.96 nm to 4.68 in NF membranes prepared from coagulation agent containing water and mixtures of water/methanol (50/50 V.%). Moreover, according to the data in Table 5, thicker membrane (107 µm) were obtained from the coagulation bath containing mixture of water/methanol (50/50 V. %) in comparison to reference membrane (100 µm).

The following points can provide more and useful insights for explanation of the effect of composition of coagulation agent on the structure and performance of NF membranes:

1) If alcohols are used as coagulant, the binodal curve in the ternary phase diagram shrinks significantly and shifts toward the coagulant–polymer axis [75]. This signifies that more coagulants are needed for casting solution to become thermodynamically unstable and reaches to binodal curve. As found in previous work [76], the delayed time increases

gradually when the coagulation bath changed from water to alcohol. This results in delayed demixing which leads to the formation of a thicker membrane with smaller pore size at the top layer and lower porosity in support layer [45].

2) As mentioned in section 3.2, polymer-solvent and solvent-coagulant interactions, and mutual diffusivity between solvent and non-solvent have great effect on membrane performance and structure. If the difference between solubility parameter of solvent and coagulant is low, the coagulant penetrate more slowly (lower mutual diffusivity between solvent and coagulant) into the cast film and delayed demixing occurs [66]. According to the solubility parameters shown in Table 2, by addition of methanol into coagulation bath, difference between solubility parameters of solvent/coagulant decreases which leads to delayed demixing [77]. From the kinetic viewpoint, it is possible to correlate the diffusional exchange of solvent/coagulants with the demixing process. Generally, higher diffusion of coagulant in solvent results in a faster precipitation. The average mutual diffusivity for intended solvent coagulant systems are tabulated in Table 3. The diffusivity coefficient between solvent and coagulant was calculated using Wilke-Chang equation (Eq. 5). The average mutual diffusivity of DMAc-water system is higher than DMAc-alcohol system. Accordingly, the lower exchange rate between solvent and methanol as coagulants leads to delayed demixing which is associated with a thicker membrane, smaller pore size at top layer and lower porosity.

3) The difference in solubility parameters between PES and the coagulants is of the order (PES–water) > (PES–(25%methanol-75%water)) > (PES–(50%methanol-50%water)). decrement in difference between solubility parameter of polymer and coagulant usually implies a slower precipitation rate which results in delayed demixing and as a consequence, a thicker membrane with lower porosity with smaller pore size is formed [78].

The contact angle of prepared membrane decreased as methanol added to coagulation bath. since the materials and dope solution composition are the same, the greater contact angle of the membrane prepared in coagulation bath containing methanol can mainly be attributed to the decreased surface porosity [64]. The addition of the methanol into coagulation bath decreases the solvent and coagulant diffusional exchange rate and hence, the average membrane surface porosity decreases and as a consequence, the wettability of the membrane decreases [61].

The effect of composition of coagulation bath on the performance of NF membranes was investigated in terms of monovalent and divalent salt rejections. Generally, increase in methanol fraction in coagulation bath led to improvements in both NaCl and $MgSO_4$ rejection of membranes. As tabulated in Table 5, the salt rejection increased form 18.62% to 25.2% for NaCl solution and from 82.78% to 91.22% for $MgSO_4$ solution when the mixture of water and methanol were employed as coagulant. The improvement in salts rejection can be explained by reduction in mean pore size of the membrane. The mean pore size of the membranes is declined when the mixtures of water and methanol were used as coagulant and the salt rejection increased due to physical size sieving, consequently.

3.5. The effect of solvent evaporation time on the properties and performance of NF membranes

The time interval between polymeric solution casting and immersion of the cast film into the coagulation bath named solvent evaporation time. This certain period significantly alters the structure and performance of the fabricated membrane. Structural analysis and characterization of membranes can provide useful information about the performance of the membranes. According to the data in Table 6, and in comparison to the reference membranes, the porosity of membranes decreased from 58.90% to 53.76% and mean pore size from 4.96 nm to 4.53 nm at 0 and 3 min solvent evaporation time, respectively. The changes in porosity and mean pore size can be attributed to the increase of polymer concentration at the top layer of the nascent film as well as the entanglement of macromolecules caused by polymer chains relaxation at longer solvent evaporation time [79]. As polymer concentration increases at the top layer, it acts as a more impenetrable barrier against the solvent outflow and coagulant inflow, which decreases diffusional exchange rate between solvent and coagulant. As a consequence, a membrane with lower porosity and smaller pore size is formed [80]. Moreover, the thickness of the membrane increased from 100 µm to 107 µm at longer solvent evaporation time. This may arise from the fact that increase of polymer concentration at the top layer of cast film provides less opportunity for the penetration of coagulation agent and accordingly less contraction ratio is provided due to the slowed demixing rate [45].

Membranes prepared at longer solvent evaporation time exhibited lower water flux. The pure water flux decreased from 38.35 lit/m^2.h to 26.73 lit/m^2.h as solvent evaporation time increased from 0 min to 3 min. The pure water flux is directly proportional with porosity and pore size and reversely with membrane thickness. At longer solvent evaporation time, the membrane porosity and pore size decreased and membrane thickness increased causing lower water flux. Increment in solvent evaporation time affects considerably the salts rejection. As tabulated in Table 6, the salts rejection increased form 18.62% to 30.65% for NaCl solution and from 82.78% to 91.58% for $MgSO_4$ solution at 0 and 3 min solvent evaporation time, respectively. It is associated to diminution of pore size improving salts rejection through both size sieving and electrostatic charge repulsion (due to increment in surface charge density) [57]. About contact angle, no clear changes can be concluded. Minor increment in contact angle by increasing solvent evaporation time may be attributed to lower surface porosity [64].

3.6. The effect of coagulation bath temperature (CBT) on the properties and performance of NF membranes

The effects of three different levels of CBT (0 °C, 20 °C, 50 °C) on membrane structure and performance are tabulated in Table 6. The pure water flux of PES NF membrane at CBT of 0 °C was 25.35 lit.m^{-2}.h^{-1}. When CBT was increased to 50 °C, the pure water flux increased largely to 52.12 lit.m^{-2}.h^{-1}. The increase of pure water flux may be attributed to three reasons. First is lower resistance caused by the thinner top layer; second is the enlarged pores on the top layer; and third is higher porosity. In general, porous structure with macrovoid occurred under instantaneous demixing condition and demixing is faster at higher temperature. On the other hand, in a lower CBT, delayed demixing occurs causing inhibited freely growth of limited nuclei on the top layer, instead many small nuclei are formed and distributed throughout the cast film. Accordingly, despite to instantaneous demixing, formation of macrovoids is suppressed and denser membranes are formed [63].

The porosity of the prepared increased from 52.89% to 65.29% and membrane thickness decreased from 111 µm to 90 µm in NF membranes prepared from coagulation bath with 0 °C and 50 °C, respectively. The Diffusivity coefficient between solvent and coagulant is temperature-dependent. According to Eq.5, increase in temperature enhances diffusional exchange rate between solvent and coagulant in the casting solution during solidification process which leads to instantaneous demixing and thus induces the formation of membrane more porous structure. Increment in diffusivity coefficient by temperature, decelerates penetration of coagulation agent and accordingly less contraction ratio is provided due to the slowed demixing rate and thicker membrane was obtained.

The CBT values have great influence on membrane performance in salts rejection. By decreasing CBT, the NaCl rejection increased from 9.25% to 31.33% and $MgSO_4$ rejection increased from 72.95% to 92.25% in NF membranes prepared from coagulation bath with 0

°C and 50 °C, respectively. Decrement the CBT can also increases the dope viscosity, the chain rigidity, and surface tension of solution which will cause slow precipitation and membrane with smaller pore size is formed [81]. As a results, the salts rejection increases.

Water contact angle improved by increasing CBT. Similar results are reported elsewhere [81]. It should be noted that the wettability of the membrane is influenced by the membrane material as well as the surface porosity and roughness. Thus, since the materials and dope solution composition are the same, the greater contact angle of the membrane prepared at higher CBT can mainly be attributed to the decreased surface porosity [64].

3.7. The effect of membrane casting speed on the properties and performance of NF membranes

Casting speed significantly affects the membrane performance and structure. The shear rate experienced during casting was calculated using the following relationship:

$$\text{Shear rate } (s^{-1}) = \frac{\text{Velocity of casting knife (m/s)}}{\text{Membrane thickness (m)}} \qquad (6)$$

According to Table 7, the membrane thickness decreased upon increase in the applied shear rate. Consequently, the pure water flux was affected by membrane thickness and increased from 25.13 lit.m^{-2}.h^{-1} to 41.32 lit.m^{-2}.h^{-1} in membrane prepared at shear rates 9.23 s^{-1} and 42.76 s^{-1}, respectively. Based on the structural data, a thinner membrane with more porosity was formed at higher shear rate resulting in higher pure water flux [55]. These findings are in agreement with literature [55, 57]. Kusworo et al. [56] reported that at higher shear rate, a decrease in dope viscosity occurs due to reduction of chain entanglement. Boussu et al. [45] claimed that at lower dope viscosity, the diffusional exchange between solvent and coagulant increases causing the formation of porous structure. Moreover, by increasing the shear rate, the pore size of the membranes was decreased. The decrement in pore size resulted in better rejection of solutes. The NaCl rejection increased from 17.12% to 23.32% and $MgSO_4$

rejection increased from 80.98% to 90.83% in NF membranes prepared at shear rates 9.23 s^{-1} and 42.76 s^{-1}, respectively. This results agree well with those reported by Ali et al. [57]. The significant betterment in salts rejection can be attributed to molecular orientation induced by shear rate during the casting of polymer film [82]. As shown in Fig. 8, macromolecules exposed to a higher shear rate tend to align more ordered than those under a lower shear rate. Enhancement in the molecular orientation causes the polymer chains to pack closer leading to decrement in free volume or pore size [57, 82, 83]. Formation of smaller pore size and increase in surface charge density of membrane (due to lower pore size) enhance the separation performance of PES NF membranes [57]. The contact angle of prepared membrane have no clear change by alteration of shear rate.

3.8. The effect of membrane thickness on the properties and performance of NF membranes

Membrane thickness plays an important role in the selective layer thickness and its pore size that determine the flux and rejection of the NF membranes. The effect of membrane thickness on pure water flux are exhibited in Table 7. The pure water flux decreased from 56.41 $lit.m^{-2}.h^{-1}$ to 17.87 $lit.m^{-2}.h^{-1}$ in membrane prepared with thickness of 100 µm and 300 µm, respectively. The results demonstrate that the membrane with lower thickness were more permeable due to lower membrane resistance, higher porosity and larger pore size. At the beginning of the phase inversion process, due to increment in the ratio of the solvent out-diffusion to the coagulant (water) inter-diffusion, the polymer concentration at the top layer may shift to a higher value. When the delay time is long, a higher polymer concentration is achieved at interphase between polymer film and coagulant bath, which leads the fast growth of the dense layer. As a result, a thicker and denser top layer with smaller pore size was formed and as consequence, the pure water flux decreased [84]. The membrane porosity decreased significantly from 63.60% to 52.91% in membrane prepared with thickness of 100 μm and 300 μm, respectively. A higher casting knife gap decelerated the diffusional exchange between solvent and coagulant and thus, the membrane structure became thicker and less porous [58]. The mean pore sizes of the membranes are tabulated in Table 7. As initial casting thickness increases, diffusion rate of coagulants in the cast films decreases and hence, delayed demixing occurs. Therefore, the mean pore size was shifted to lower value as the membrane thickness increased [58].

The effect of casting solution thickness on rejection is depicted in Table 7. By increasing membrane thickness, the NaCl rejection increased from 17.12% to 23.32% and $MgSO_4$ rejection increased from 80.98% to 90.83% in NF membranes prepared with thickness of 100 μm and 300 μm, respectively. The decrement of pore size enhances the salts rejection through both size sieving and electrostatic repulsion mechanisms. As membrane thickness increased, the contact angle decreased. since the materials and dope solution are the same, the greater contact angle of the thicker membrane can mainly be attributed to the decreased surface porosity [64]

3.9. Effect of operating parameters on the properties and performance of NF membranes

3.9.1. Feed pressure

The effect of feed pressure on water flux and salts rejection of reference membrane (PES/DMAc 76%/24%) is shown in Fig. 9. Due to porous nature of the membrane, the Hagen–Poiseuille equation can be considered under the hypothesis of constant pressure gradient along the membrane pore [85]. According to the Hagen–Poiseuille flow as expressed in Eq. (7), increase in water flux is proportional to the increase in pressure difference across the membrane.

$$J_V = \frac{r_p^2}{8\eta\delta}\,\Delta P = L_p\,\Delta P \qquad (7)$$

Where J_V (m.s^{-1}), r_p (m), η (Pa.s^{-1}), δ (m), ΔP (Pa) and L_p (m.s^{-1}.Pa^{-1}) are volume flux, average pore radius, water dynamic viscosity inside the pore, effective membrane thickness, pressure difference across the membrane and, hydraulic membrane permeability, respectively. According to Fig. 9 (a), water flux data versus feed pressure is approximately linear and water permeability for are calculated about 16.47 lit.m^2.h^{-1}.bar^{-1}. Also, the salts rejection increased with the increase in feed pressure (Fig. 9 (b)). This is due to the water permeate flux through the membrane is linearly related to the trans-membrane pressure, whereas the salt flux is relevant to the both concentration gradient across the membrane and the water flux. When the feed pressure increases, the water permeate flux increases relatively more as compared to the salt permeate. This causes a decreasing salt concentration in permeate stream and an increasing rejection [86].

3.9.2. Feed pH

The salt rejection and water flux as a function of feed pH were investigated for reference membrane (PES/DMAc 76%/24%) and the results are exhibited in Table 8. Zeta potential of the membranes was also measured to determine the membrane surface charge. Fig. 10 shows the zeta potential of membranes as a function of pH. Higher zeta potential of PES membrane at higher solution pH value indicates more negative the membrane surface. It is believed that the negative charge of the PES membrane originates from the functional groups of PES (O=S=O) [74]. Due to the electrostatic charge repulsion between SO_4^{2-} and Cl^- molecules and negative charges on the membrane surface, SO_4^{2-} and Cl^- molecules are rejected. Increment in solution pH results in an increment in the negative surface charge of membrane which leads to stronger electrostatic charge repulsion between anions and membrane surface and increases the rejection of anions. Subsequently, the rejection of cations (Mg^{2+}, Na^{+}) increases due to Donnan effect. In other words, if anions (SO_4^{2-} and Cl^{-}) are rejected because of electrostatic charge repulsion with negative surface charge of PES membrane, then the cations will also have to be rejected to neutralize electric charge across the membrane. For salts, an increase in co-ion charge and a decrease in counter ion charge improve salts rejection [65]. Because of higher charge of sulfate ions, the rejection of Mg^{2+} ions also increases due to Donnan effect. The electrostatic charge repulsion between anions molecules and membrane surface increases by increasing the solution pH, which hinders anions molecules to adsorb on the membrane surface. As adsorption of anions molecules on membrane surface decreases, the barriers for the solution passage across the membrane decreases and therefore water flux increases [72].

3.10. Comparison with literature

Table 9 provides the salt rejection and water flux performance of several commercial and non-commercial NF membranes reported in literatures. It can be seen that the water flux for the membranes developed in this study were almost higher than others in the Table, except that of NF90. This can be attributed to high porosity, low thickness and formation of more free volume in the structure of developed membranes. On the other hand, the salts rejection performance of fabricated membranes seems to be satisfactory by consideration of salt concentration used for testing in comparison with other works. The membrane performance for divalent ions was better than monovalent ions. Authors are working for further improvements in this respect.

4. Conclusions

The properties and performance of asymmetric PES NF membranes were investigated and through systematics analysis of the effect of design, fabrication and operational parameters with the main aim of obtaining membranes with high rejection of monovalent and divalent salt while possessing reasonable water flux. Results revealed that among the studied parameters, polymer concentration greatly affected membrane morphology and performance. Besides, it was found that the membrane structure and performance were considerably dependent solvent-coagulating agent and solvent-polymer interactions. In overall, membranes prepared using DMAc exhibited a higher water flux than those prepared using NMP as solvent. Modified membranes containing organic acids exhibited structures with lower thickness, higher porosity and smaller pore size compared to unmodified membrane attributed to the hydrophilic functional groups of additives proven by the water contact angle data displaying that the wettability of membranes increased by both citric and ascorbic acids. The water flux of modified membrane improved by addition of 1 wt% of organic acids, though the salts rejection improved for all concentrations of organic acids. Structural analysis of the membranes indicated that the membranes prepared with coagulant containing methanol had lower porosity, smaller pore size, less hydrophilic surface and higher thickness due to slower diffusional exchange between solvent and coagulant. Despite the decline in pure water flux, both NaCl and $MgSO_4$ rejection were improved in membranes prepared using water/methanol mixture as coagulating agent. Moreover, derived membranes from lower temperature, higher thickness and higher solvent evaporation time were found less porous with lower mean pore size and less permeable to water and more capable to salts rejection. In all membrane due to negative surface charge of PES membrane, the rejection of divalent ions was greater than monovalent ion. As a consequence, addition of organic acids and increment in casting shear rate simultaneously improved both water flux and salt rejection, but there is a trade-off between selectivity and permeability for alteration of other parameters. The findings provide valuable information and guidelines for development of high performance nanofiltration membranes for specialized separation applications.

Acknowledgements

Authors would like to thank Iran Nanotechnology Initiative Council (INIC) for partial financial support to this project.

Re[87]f[88]erences [89]

References

[1] Y. Xiao, B. T. Low, S. S. Hosseini, T. S. Chung, and D. R. Paul, "The strategies of molecular architecture and modification of polyimide-based membranes for CO2 removal from natural gas—A review," *Progress in Polymer Science,* vol. 34, pp. 561-580, 2009.

[2] S. S. Hosseini and T. S. Chung, "Carbon membranes from blends of PBI and polyimides for N2/CH4 and CO2/CH4 separation and hydrogen purification," *Journal of Membrane Science,* vol. 328, pp. 174-185, 2009.

[3] S. S. Hosseini, M. M. Teoh, and T. S. Chung, "Hydrogen separation and purification in membranes of miscible polymer blends with interpenetration networks," *Polymer,* vol. 49, pp. 1594-1603, 2008.

[4] S. Ü. Çelik, A. Bozkurt, and S. S. Hosseini, "Alternatives toward proton conductive anhydrous membranes for fuel cells: Heterocyclic protogenic solvents comprising polymer electrolytes," *Progress in Polymer Science,* vol. 37, pp. 1265-1291, 9// 2012.

[5] M. Tamaddondar, H. Pahlavanzadeh, S. Saeid Hosseini, G. Ruan, and N. R. Tan, "Self-assembled polyelectrolyte surfactant nanocomposite membranes for pervaporation separation of MeOH/MTBE," *Journal of Membrane Science,* vol. 472, pp. 91-101, 12/15/ 2014.

[6] S. S. Hosseini, Y. Li, T.-S. Chung, and Y. Liu, "Enhanced gas separation performance of nanocomposite membranes using MgO nanoparticles," *Journal of Membrane Science,* vol. 302, pp. 207-217, 2007.

[7] S. S. Hosseini, M. R. Omidkhah, A. Zarringhalam Moghaddam, V. Pirouzfar, W. B. Krantz, and N. R. Tan, "Enhancing the properties and gas separation performance of PBI–polyimides blend carbon molecular sieve membranes via optimization of the pyrolysis process," *Separation and Purification Technology,* vol. 122, pp. 278-289, 2014.

[8] S. S. Hosseini, N. Peng, and T. S. Chung, "Gas separation membranes developed through integration of polymer blending and dual-layer hollow fiber spinning process for hydrogen and natural gas enrichments," *Journal of Membrane Science,* vol. 349, pp. 156-166, 2010.

[9] V. Pirouzfar, S. S. Hosseini, M. R. Omidkhah, and A. Z. Moghaddam, "Modeling and optimization of gas transport characteristics of carbon molecular sieve membranes through statistical analysis," *Polymer Engineering & Science,* pp. n/a-n/a, 2013.

[10] V. Pirouzfar, A. Z. Moghaddam, M. R. Omidkhah, and S. S. Hosseini, "Investigating the effect of dianhydride type and pyrolysis condition on the gas separation

performance of membranes derived from blended polyimides through statistical analysis," *Journal of Industrial and Engineering Chemistry,* 2013.

[11] W. B. Krantz, A. R. Greenberg, E. Kujundzic, A. Yeo, and S. S. Hosseini, "Evapoporometry: A novel technique for determining the pore-size distribution of membranes," *Journal of Membrane Science,* vol. 438, pp. 153-166, 7/1/ 2013.

[12] S. S. Hosseini, S. M. Roodashti, P. K. Kundu, and N. R. Tan, "Transport Properties of Asymmetric Hollow Fiber Membrane Permeators for Practical Applications: Mathematical Modeling For Binary Gas Mixtures," *Canad. J. Chem. Eng., In Press.*

[13] I. Koyuncu and M. Cakmakci, "Nanofiltration for Water and Wastewater Treatment," *Nanotechnology in Water Treatment Applications,* p. 103, 2010.

[14] B. A. M. Al-Rashdi, D. J. Johnson, and N. Hilal, "Removal of heavy metal ions by nanofiltration," *Desalination,* vol. 315, pp. 2-17, 2013.

[15] A. Rahimpour, M. Jahanshahi, N. Mortazavian, S. S. Madaeni, and Y. Mansourpanah, "Preparation and characterization of asymmetric polyethersulfone and thin-film composite polyamide nanofiltration membranes for water softening," *Applied Surface Science,* vol. 256, pp. 1657-1663, 2010.

[16] A. R. Anim-Mensah, W. B. Krantz, and R. Govind, "Studies on polymeric nanofiltration-based water softening and the effect of anion properties on the softening process," *European Polymer Journal,* vol. 44, pp. 2244-2252, 2008.

[17] B. Van der Bruggen and C. Vandecasteele, "Removal of pollutants from surface water and groundwater by nanofiltration: overview of possible applications in the drinking water industry," *Environmental Pollution,* vol. 122, pp. 435-445, 2003.

[18] N. Hilal, H. Al-Zoubi, N. A. Darwish, A. W. Mohamma, and M. Abu Arabi, "A comprehensive review of nanofiltration membranes: Treatment, pretreatment, modelling, and atomic force microscopy," *Desalination,* vol. 170, pp. 281-308, 2004.

[19] M. Telzhensky, L. Birnhack, O. Lehmann, E. Windler, and O. Lahav, "Selective separation of seawater Mg< sup> 2+</sup> ions for use in downstream water treatment processes," *Chemical Engineering Journal,* vol. 175, pp. 136-143, 2011.

[20] A. Lhassani, M. Rumeau, D. Benjelloun, and M. Pontie, "Selective demineralization of water by nanofiltration application to the defluorination of brackish water," *Water research,* vol. 35, pp. 3260-3264, 2001.

[21] K. Walha, R. B. Amar, L. Firdaous, F. Quéméneur, and P. Jaouen, "Brackish groundwater treatment by nanofiltration, reverse osmosis and electrodialysis in Tunisia: performance and cost comparison," *Desalination,* vol. 207, pp. 95-106, 2007.

[22] S. Zhao, L. Zou, and D. Mulcahy, "Brackish water desalination by a hybrid forward osmosis–nanofiltration system using divalent draw solute," *Desalination,* vol. 284, pp. 175-181, 2012.

[23] S. Chakraborty, M. K. Purkait, S. DasGupta, S. De, and J. K. Basu, "Nanofiltration of textile plant effluent for color removal and reduction in COD," *Separation and purification Technology,* vol. 31, pp. 141-151, 2003.

[24] S. K. Nataraj, K. M. Hosamani, and T. M. Aminabhavi, "Nanofiltration and reverse osmosis thin film composite membrane module for the removal of dye and salts from the simulated mixtures," *Desalination,* vol. 249, pp. 12-17, 2009.

[25] B. M. Watson and C. D. Hornburg, "Low-energy membrane nanofiltration for removal of color, organics and hardness from drinking water supplies," *Desalination,* vol. 72, pp. 11-22, 1989.

[26] M. Barakat, "New trends in removing heavy metals from industrial wastewater," *Arabian Journal of Chemistry,* vol. 4, pp. 361-377, 2011.

[27] M. Muthukrishnan and B. Guha, "Effect of pH on rejection of hexavalent chromium by nanofiltration," *Desalination,* vol. 219, pp. 171-178, 2008.

[28] Y. Sato, M. Kang, T. Kamei, and Y. Magara, "Performance of nanofiltration for arsenic removal," *Water Research,* vol. 36, pp. 3371-3377, 2002.

[29] A. P. Echavarria, C. Torras, J. Pagán, and A. Ibarz, "Fruit juice processing and membrane technology application," *Food Engineering Reviews,* vol. 3, pp. 136-158, 2011.

[30] L. D. Nghiem, A. I. Schäfer, and M. Elimelech, "Pharmaceutical retention mechanisms by nanofiltration membranes," *Environmental science & technology,* vol. 39, pp. 7698-7705, 2005.

[31] B. S. Lalia, V. Kochkodan, R. Hashaikeh, and N. Hilal, "A review on membrane fabrication: Structure, properties and performance relationship," *Desalination,* vol. 326, pp. 77-95, 2013.

[32] a. Brunetti, S. Simone, F. Scura, G. Barbieri, a. Figoli, and E. Drioli, "Hydrogen mixture separation with PEEK-WC asymmetric membranes," *Separation and Purification Technology,* vol. 69, pp. 195-204, 2009.

[33] A. F. Ismail and A. R. Hassan, "Formation and characterization of asymmetric nanofiltration membrane: effect of shear rate and polymer concentration," *Journal of membrane science,* vol. 270, pp. 57-72, 2006.

[34] A. Ismail and A. Hassan, "Formation and characterization of asymmetric nanofiltration membrane: effect of shear rate and polymer concentration," *Journal of membrane science,* vol. 270, pp. 57-72, 2006.

[35] S. Yu, M. Liu, M. Ma, M. Qi, Z. Lü, and C. Gao, "Impacts of membrane properties on reactive dye removal from dye/salt mixtures by asymmetric cellulose acetate and composite polyamide nanofiltration membranes," *Journal of Membrane Science,* vol. 350, pp. 83-91, 2010.

[36] M. Buonomenna, L. Lopez, P. Favia, R. d'Agostino, A. Gordano, and E. Drioli, "New PVDF membranes: the effect of plasma surface modification on retention in nanofiltration of aqueous solution containing organic compounds," *Water research,* vol. 41, pp. 4309-4316, 2007.

[37] A. G. Fane, C. Y. Tang, and R. Wang, "4.11 - Membrane Technology for Water: Microfiltration, Ultrafiltration, Nanofiltration, and Reverse Osmosis," in *Treatise on Water Science*, W. Editor-in-Chief: Peter, Ed., ed. Oxford: Elsevier, 2011, pp. 301-335.

[38] V. Vatanpour, S. S. Madaeni, L. Rajabi, S. Zinadini, and A. A. Derakhshan, "Boehmite nanoparticles as a new nanofiller for preparation of antifouling mixed matrix membranes," *Journal of Membrane Science,* vol. 401, pp. 132-143, 2012.

[39] S. Balta, A. Sotto, P. Luis, L. Benea, B. Van der Bruggen, and J. Kim, "A new outlook on membrane enhancement with nanoparticles: the alternative of ZnO," *Journal of Membrane Science,* vol. 389, pp. 155-161, 2012.

[40] C. Zhao, J. Xue, F. Ran, and S. Sun, "Modification of polyethersulfone membranes – A review of methods," *Progress in Materials Science,* vol. 58, pp. 76-150, 2013.

[41] A. L. Ahmad, A. A. Abdulkarim, B. S. Ooi, and S. Ismail, "Recent development in additives modifications of polyethersulfone membrane for flux enhancement," *Chemical Engineering Journal,* vol. 223, pp. 246-267, 2013.

[42] P. Daraei, S. S. Madaeni, N. Ghaemi, H. A. Monfared, and M. A. Khadivi, "Fabrication of PES nanofiltration membrane by simultaneous use of multi-walled carbon nanotube and surface graft polymerization method: Comparison of MWCNT and PAA modified MWCNT," *Separation and Purification Technology,* vol. 104, pp. 32-44, 2013.

[43] J. Zhu, Y. Zhang, M. Tian, and J. Liu, "Fabrication of a Mixed Matrix Membrane with in Situ Synthesized Quaternized Polyethylenimine Nanoparticles for Dye

Purification and Reuse," *ACS Sustainable Chemistry & Engineering,* vol. 3, pp. 690-701, 2015.

[44] M. Sadrzadeh and S. Bhattacharjee, "Rational design of phase inversion membranes by tailoring thermodynamics and kinetics of casting solution using polymer additives," *Journal of Membrane Science,* vol. 441, pp. 31-44, 2013.

[45] K. Boussu, C. Vandecasteele, and B. Van der Bruggen, "Study of the characteristics and the performance of self-made nanoporous polyethersulfone membranes," *Polymer,* vol. 47, pp. 3464-3476, 2006.

[46] S. S. Madaeni and a. H. Taheri, "Preparation of PES ultrafiltration membrane for treatment of emulsified oily wastewater: Effect of solvent and non-solvent on morphology and performance," *Journal of Polymer Engineering,* vol. 29, pp. 183-198, 2009.

[47] S. S. Madaeni and a. Rahimpour, "Effect of type of solvent and non-solvents on morphology and performance of polysulfone and polyethersulfone ultrafiltration membranes for milk concentration," *Polymers for Advanced Technologies,* vol. 16, pp. 717-724, 2005.

[48] S. Madaeni and A. Rahimpour, "Effect of type of solvent and non-solvents on morphology and performance of polysulfone and polyethersulfone ultrafiltration membranes for milk concentration," *Polymers for advanced technologies,* vol. 16, pp. 717-724, 2005.

[49] K. J. Baik, J. Y. Kim, J. S. Lee, S. C. Kim, and H. K. Lee, "Morphology of membranes formed from polysulfone/polyethersulfone/N-methyl-2-pyrrolidone/water system by immersion precipitation," *Korea Polymer Journal,* vol. 9, pp. 285-291, 2001.

[50] M. Khayet, C. Cojocaru, and M. García-Payo, "Experimental design and optimization of asymmetric flat-sheet membranes prepared for direct contact membrane distillation," *Journal of Membrane Science,* vol. 351, pp. 234-245, 2010.

[51] D. Mosqueda-Jimenez, R. Narbaitz, T. Matsuura, G. Chowdhury, G. Pleizier, and J. Santerre, "Influence of processing conditions on the properties of ultrafiltration membranes," *Journal of membrane science,* vol. 231, pp. 209-224, 2004.

[52] M. Amirilargani, E. Saljoughi, T. Mohammadi, and M. R. Moghbeli, "Effects of coagulation bath temperature and polyvinylpyrrolidone content on flat sheet asymmetric polyethersulfone membranes," *Polymer Engineering & Science,* vol. 50, pp. 885-893, 2010.

[53] B. K. Chaturvedi, A. K. Ghoshb, V. Ramachandhranb, M. K. Trivedi, M. S. Hantab, and B. M. Misrab, "Preparation , characterization and performance of polyethersulfone ultrafiltration membranes," vol. 133, 2001.

[54] C. B. Spricigo, J. C. C. Petrus, R. A. F. Machado, L. A. V. Sarmento, and A. Bolzan, "Preparation and characterization of polyethersulfone membranes for use in supercritical medium," *Journal of membrane science,* vol. 205, pp. 273-278, 2002.

[55] A. F. Ismail, A. R. Hassan, and B. C. Ng, "Effect of shear rate on the performance of nanofiltration membrane for water desalination," *Songklanakarin Journal Science and Technology,* vol. 24, pp. 879-889, 2002.

[56] T. D. Kusworo, A. F. Ismail, A. Mustafa, and T. Matsuura, "Dependence of membrane morphology and performance on preparation conditions: The shear rate effect in membrane casting," *Separation and Purification Technology,* vol. 61, pp. 249-257, 2008.

[57] N. A. Ali, N. Halim, A. Jusoh, and A. Endut, "The formation and characterisation of an asymmetric nanofiltration membrane for ammonia–nitrogen removal: Effect of shear rate," *Bioresource technology,* vol. 101, pp. 1459-1465, 2010.

[58] A. Ahmad, N. Ideris, B. Ooi, S. Low, and A. Ismail, "Synthesis of polyvinylidene fluoride (PVDF) membranes for protein binding: Effect of casting thickness," *Journal of Applied Polymer Science,* vol. 128, pp. 3438-3445, 2013.

[59] A. Conesa, T. Gumí, and C. Palet, "Membrane thickness and preparation temperature as key parameters for controlling the macrovoid structure of chiral activated membranes (CAM)," *Journal of membrane science,* vol. 287, pp. 29-40, 2007.

[60] N. Vogrin, Č. Stropnik, V. Musil, and M. Brumen, "The wet phase separation: the effect of cast solution thickness on the appearance of macrovoids in the membrane forming ternary cellulose acetate/acetone/water system," *Journal of membrane science,* vol. 207, pp. 139-141, 2002.

[61] A. Sotto, A. Boromand, S. Balta, J. Kim, and B. Van der Bruggen, "Doping of polyethersulfone nanofiltration membranes: antifouling effect observed at ultralow concentrations of TiO 2 nanoparticles," *Journal of Materials Chemistry,* vol. 21, pp. 10311-10320, 2011.

[62] V. Vatanpour, S. S. Madaeni, R. Moradian, S. Zinadini, and B. Astinchap, "Novel antibifouling nanofiltration polyethersulfone membrane fabricated from embedding TiO< sub> 2</sub> coated multiwalled carbon nanotubes," *Separation and Purification Technology,* vol. 90, pp. 69-82, 2012.

[63] M. Amirilargani, E. Saljoughi, T. Mohammadi, and M. Moghbeli, "Effects of coagulation bath temperature and polyvinylpyrrolidone content on flat sheet asymmetric polyethersulfone membranes," *Polymer Engineering & Science,* vol. 50, pp. 885-893, 2010.

[64] M. Omidvar, S. mahmoud Mousavi, M. Soltanieh, and A. A. Safekordi, "Preparation and characterization of poly (ethersulfone) nanofiltration membranes for amoxicillin removal from contaminated water," *Journal of Environmental Health Science and Engineering,* vol. 12, pp. 1-10, 2014.

[65] T. Dey, *Nanotechnology for water purification*: Universal-Publishers, 2012.

[66] S. Madaeni and A. Taheri, "Preparation of PES ultrafiltration membrane for treatment of emulsified oily wastewater: Effect of solvent and non-solvent on morphology and performance," *Journal of Polymer Engineering,* vol. 29, pp. 183-198, 2009.

[67] K.-Y. Chun, S.-H. Jang, H.-S. Kim, Y.-W. Kim, H.-S. Han, and Y.-i. Joe, "Effects of solvent on the pore formation in asymmetric 6FDA–4, 4′ ODA polyimide membrane: terms of thermodynamics, precipitation kinetics, and physical factors," *Journal of Membrane Science,* vol. 169, pp. 197-214, 2000.

[68] L. Wang, Z. Li, J. Ren, S.-G. Li, and C. Jiang, "Preliminary studies on the gelation time of poly (ether sulfones) membrane-forming system with an elongation method," *Journal of membrane science,* vol. 275, pp. 46-51, 2006.

[69] J. Barzin and B. Sadatnia, "Correlation between macrovoid formation and the ternary phase diagram for polyethersulfone membranes prepared from two nearly similar solvents," *Journal of Membrane Science,* vol. 325, pp. 92-97, 2008.

[70] H. Hasbullah, A. F. Ismail, B. Ng, and M. Abdullah, "Effect of solvent types on structure and performance of polyethersulfone nanofiltration membrane in monovalent and divalent ions separation," 2005.

[71] M. Ghosh, *Polyimides: fundamentals and applications*: CRC Press, 1996.

[72] N. Ghaemi, S. S. Madaeni, A. Alizadeh, P. Daraei, M. M. S. Badieh, M. Falsafi*, et al.*, "Fabrication and modification of polysulfone nanofiltration membrane using organic acids: Morphology, characterization and performance in removal of xenobiotics," *Separation and Purification Technology,* vol. 96, pp. 214-228, 2012.

[73] I. C. Kim and K. H. Lee, "Effect of various additives on pore size of polysulfone membrane by phase-inversion process," *Journal of applied polymer science,* vol. 89, pp. 2562-2566, 2003.

[74] V. Vatanpour, M. Esmaeili, and M. H. D. A. Farahani, "Fouling reduction and retention increment of polyethersulfone nanofiltration membranes embedded by amine-functionalized multi-walled carbon nanotubes," *Journal of Membrane Science,* vol. 466, pp. 70-81, 2014.

[75] B. T. Swinyard and J. A. Barrie, "Phase separation in non-solvent/dimethylformamide/polyethersulphone and non-solvent/dimethylformamide/polysulphone systems," *British polymer journal,* vol. 20, pp. 317-321, 1988.

[76] D.-y. Zuo, B.-k. Zhu, J.-h. Cao, and Y.-y. Xu, "Influence of alcohol-based nonsolvents on the formation and morphology of PVDF membranes in phase inversion process," *Chinese journal of polymer science,* vol. 24, pp. 281-289, 2006.

[77] A. Rahimpour, S. S. Madaeni, M. Jahanshahi, Y. Mansourpanah, and N. Mortazavian, "Development of high performance nano-porous polyethersulfone ultrafiltration membranes with hydrophilic surface and superior antifouling properties," *Applied Surface Science,* vol. 255, pp. 9166-9173, 2009.

[78] P. Sukitpaneenit and T.-S. Chung, "Molecular elucidation of morphology and mechanical properties of PVDF hollow fiber membranes from aspects of phase inversion, crystallization and rheology," *Journal of Membrane Science,* vol. 340, pp. 192-205, 2009.

[79] M. Khayet and T. Matsuura, *Membrane distillation: principles and applications*: Elsevier, 2011.

[80] C. Feng, B. Shi, G. Li, and Y. Wu, "Preparation and properties of microporous membrane from poly (vinylidene fluoride-co-tetrafluoroethylene)(F2. 4) for membrane distillation," *Journal of membrane science,* vol. 237, pp. 15-24, 2004.

[81] Y. Wang, B. Shi, and X. Li, "Effects of coagulation bath temperature on performances of polyethersulfone membranes modified by nanosilver particles in situ reduction," *Polymer Engineering & Science,* vol. 53, pp. 1614-1622, 2013.

[82] T.-S. Chung, S. K. Teoh, W. W. Y. Lau, and M. P. Srinivasan, "Effect of shear stress within the spinneret on hollow fiber membrane morphology and separation performance," *Industrial & engineering chemistry research,* vol. 37, pp. 3930-3938, 1998.

[83] C. Cao, T.-S. Chung, S. B. Chen, and Z. Dong, "The study of elongation and shear rates in spinning process and its effect on gas separation performance of poly (ether sulfone)(PES) hollow fiber membranes," *Chemical engineering science,* vol. 59, pp. 1053-1062, 2004.

[84] S. Zhang, K. Y. Wang, T.-S. Chung, Y. C. Jean, and H. Chen, "Molecular design of the cellulose ester-based forward osmosis membranes for desalination," *Chemical Engineering Science,* vol. 66, pp. 2008-2018, 2011.

[85] S. Bandini and L. Bruni, "Transport phenomena in nanofiltration membranes," *Comprehensive Membrane Science and Engineering, Elsevier, Oxford,* pp. 67-89, 2010.

[86] K. Y. Wang, Y. Xiao, and T.-S. Chung, "Chemically modified polybenzimidazole nanofiltration membrane for the separation of electrolytes and cephalexin," *Chemical Engineering Science,* vol. 61, pp. 5807-5817, 2006.

[87] A. Somrani, A. Hamzaoui, and M. Pontie, "Study on lithium separation from salt lake brines by nanofiltration (NF) and low pressure reverse osmosis (LPRO)," *Desalination,* vol. 317, pp. 184-192, 2013.

[88] M. Telzhensky, L. Birnhack, O. Lehmann, E. Windler, and O. Lahav, "Selective separation of seawater Mg2+ ions for use in downstream water treatment processes," *Chemical Engineering Journal,* vol. 175, pp. 136-143, 11/15/ 2011.

[89] V. Vatanpour, S. S. Madaeni, R. Moradian, S. Zinadini, and B. Astinchap, "Fabrication and characterization of novel antifouling nanofiltration membrane prepared from oxidized multiwalled carbon nanotube/polyethersulfone nanocomposite," *Journal of Membrane Science,* vol. 375, pp. 284-294, 2011.

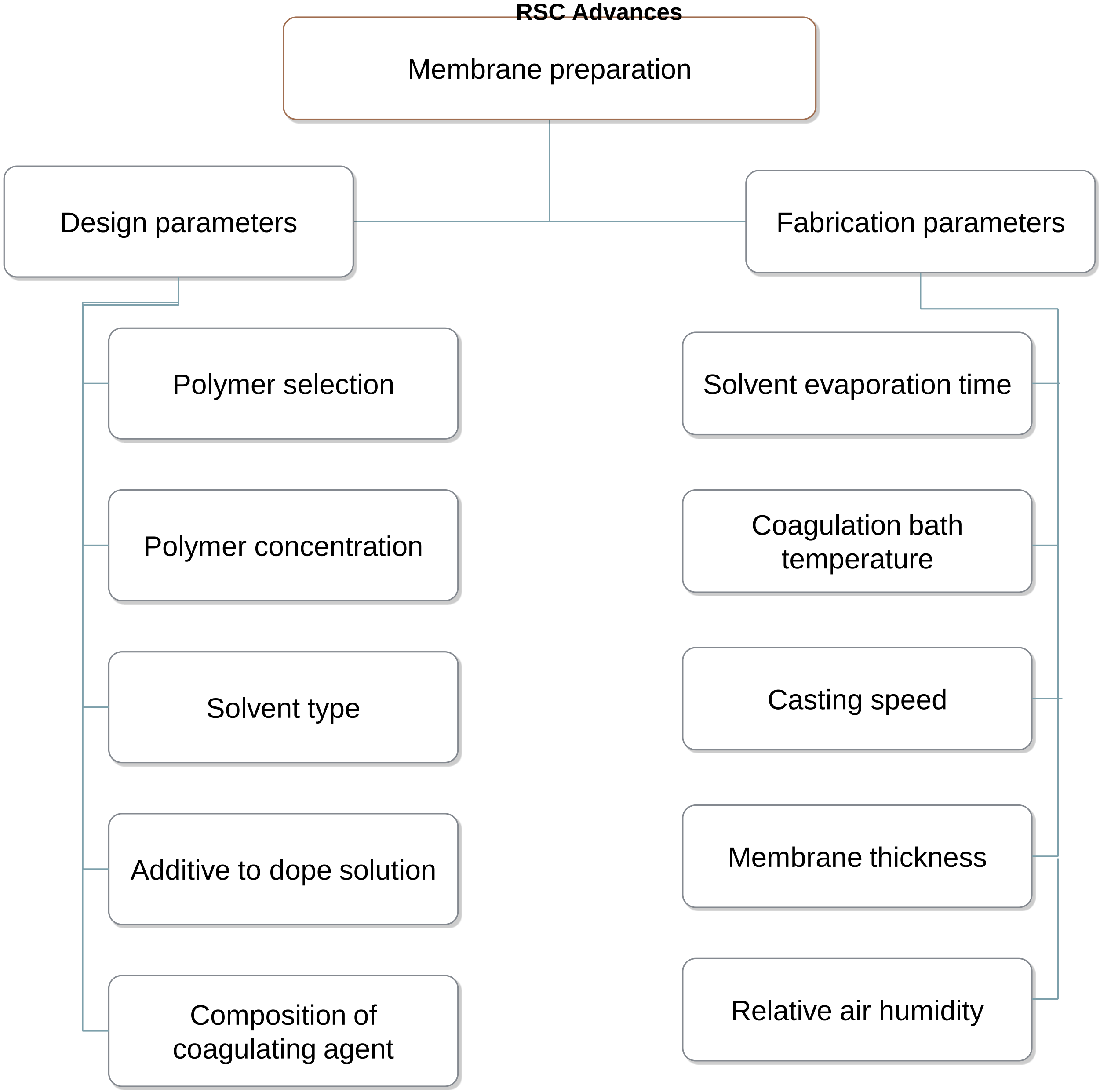

Fig. 1. Classification of prominent design and fabrication parameters involved in preparation of asymmetric membranes.

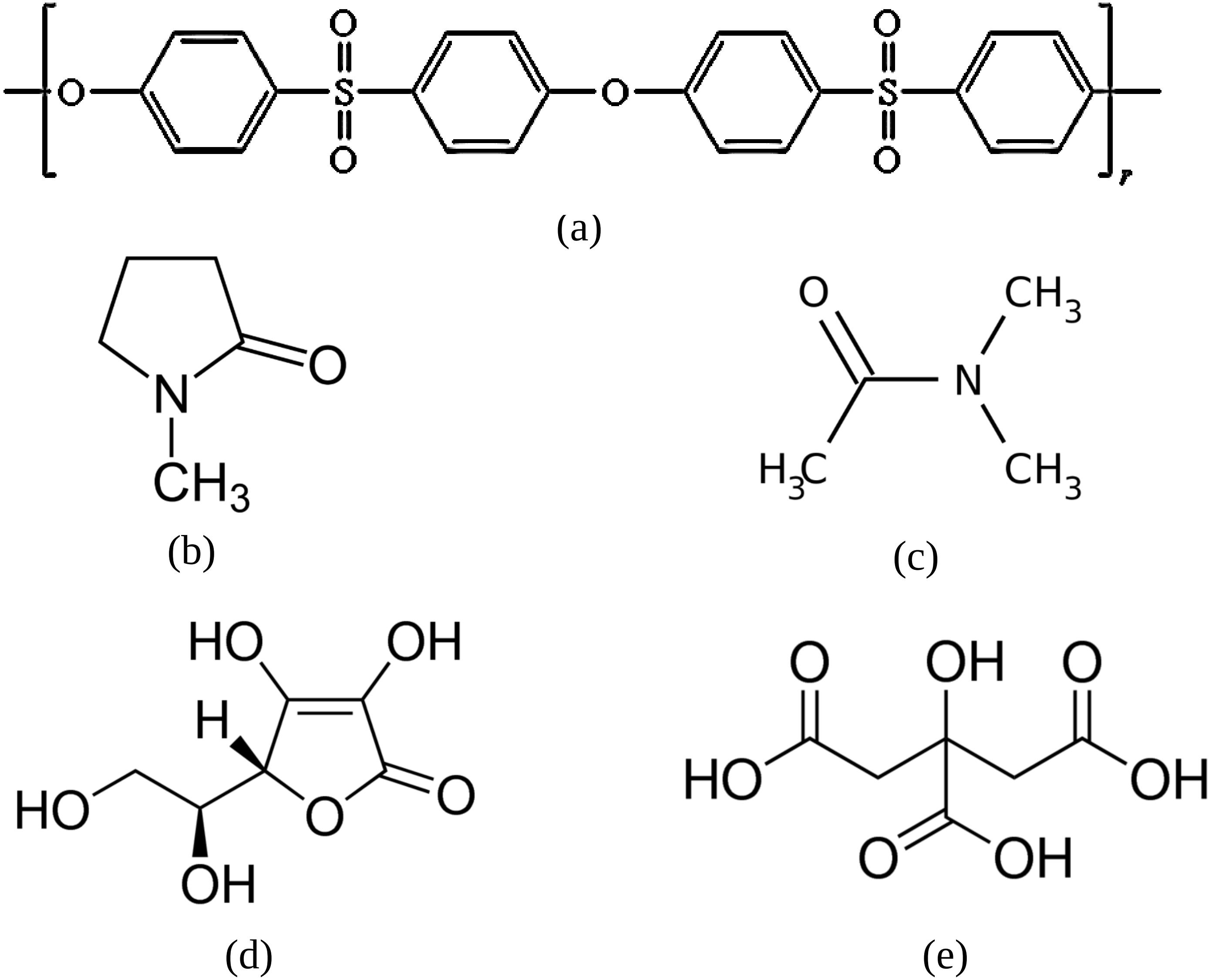

Fig. 2. Chemical structures of (a) PES (b) NMP (c) DMAc (d) Ascorbic acid (e) Citric acid.

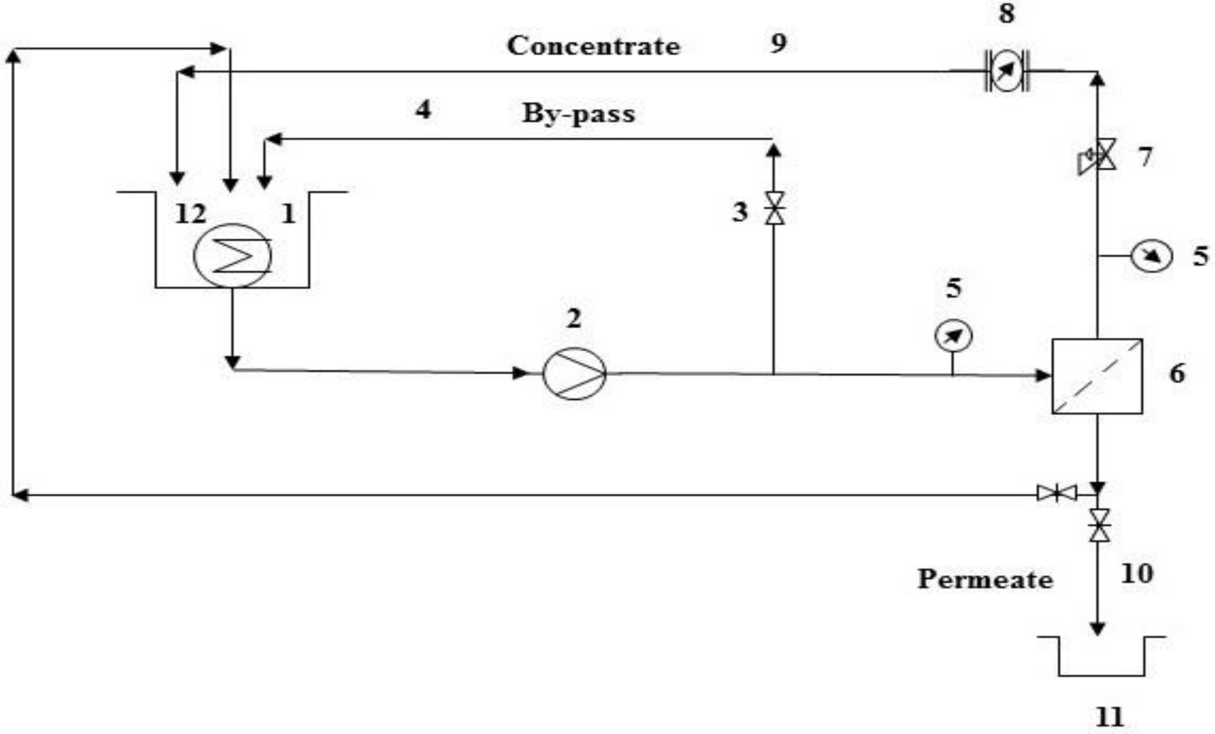

Fig. 3. Cross-flow filtration system: (1) Feed tank (2) Pump (3) Valve (4) By-pass stream (5) Pressure gauge (6) Membrane madule (7) Back-pressure regulator (8) Flowmeter (9) Retentate stream (10) Permeate (11) Permeate tank (12) Cooling system

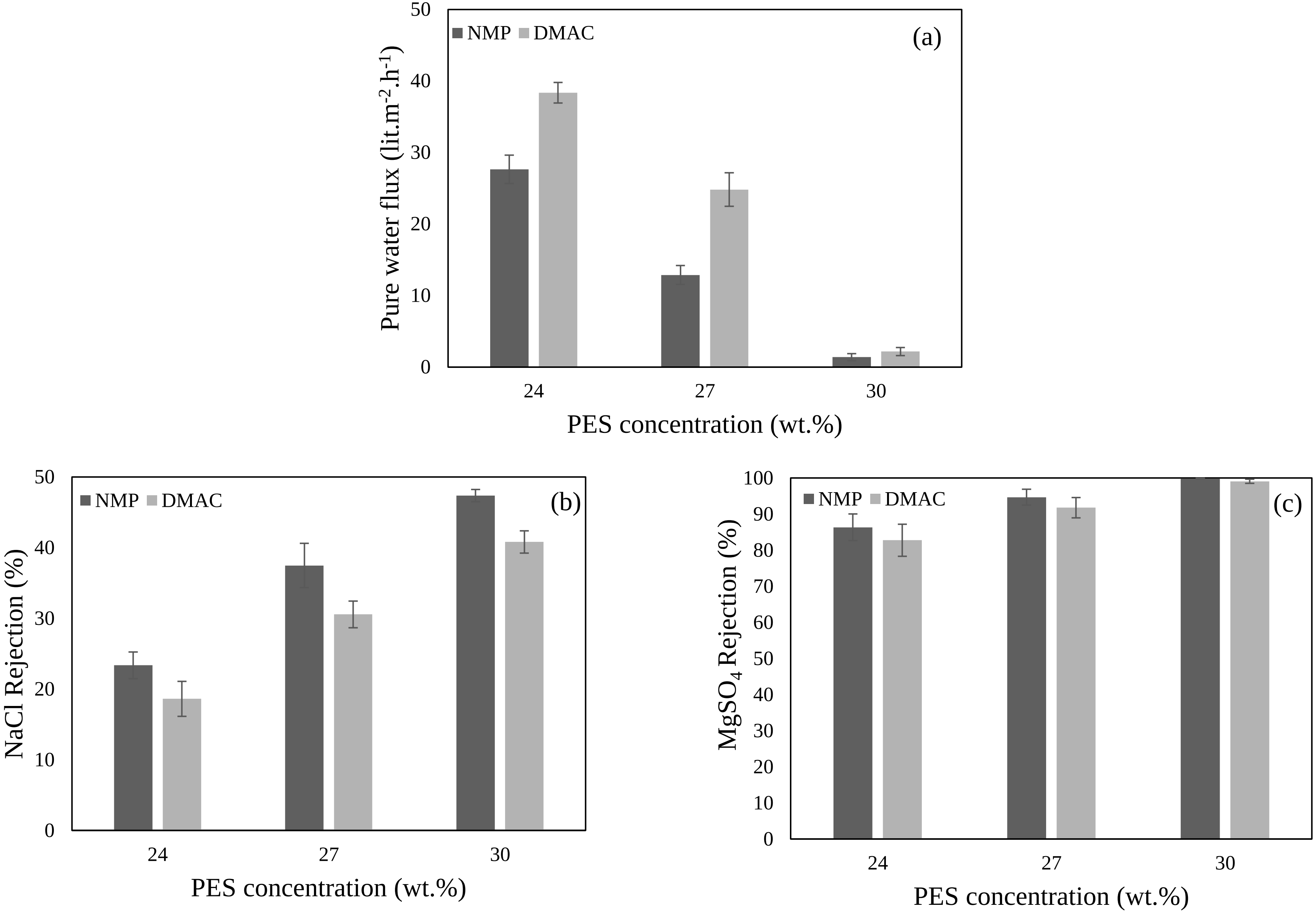

Fig. 4. The effect of PES concentration in the dope solution on (a) pure water flux (b) NaCl rejection (c) $MgSO_4$ rejection of NF membranes prepared using NMP and DMAc as solvents.

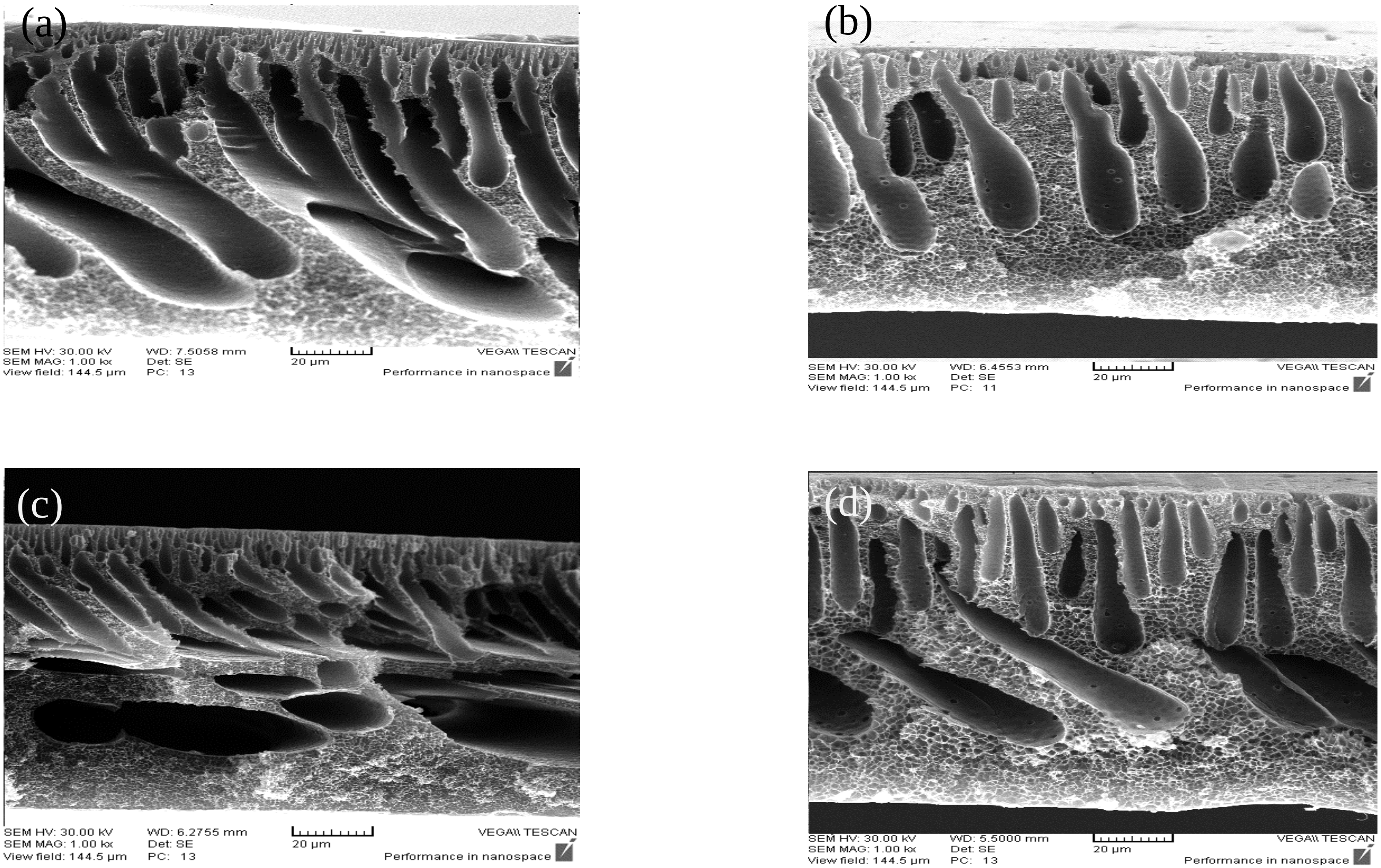

Fig. 5. Cross section SEM images of PES NF membranes: (a) Polymer concentration: 24 wt%.; Solvent: NMP, (b) Polymer concentration: 30 wt%.; Solvent: NMP, (c) Polymer concentration: 24 wt%.; Solvent: DMAc, (d) Polymer concentration: 30 wt%.; Solvent: DMAc.

Table 1. The effect of solvent type and polymer concentration in dope on the characteristics of the PES NF membranes*.

Solvent	Polymer concentration (wt.%)	Membrane thickness (µm)	Mean pore size (nm)	Porosity (%)	Area fraction of macrovoids (%)	Contact angle (°)
NMP	24	125	4.93	55.5	54.96	63.4
	27	130	3.19	52.3	-	72.6
	30	133	1.20	46.2	40.58	75.5
DMAc	24	100	4.96	58.9	65.78	60.5
	27	107	4.09	55.7	-	67.3
	30	111	1.64	47.6	48.54	72.9

* Conditions: Casting temperature: 25±3° C; Relative air humidity: 30±5%; Casting knife gap: 200 µm; Casting shear rate: 23.54 s^{-1}; Solvent evaporation time: 0 min; Coagulating agent: pure water; Coagulation bath temperature: 20±2° C.

Table 2. Solubility parameters of the materials and compounds used in this study.

Material/ Compound	**Solubility parameter ($MPa^{0.5}$)**			
	$\boldsymbol{\delta_d}$	$\boldsymbol{\delta_p}$	$\boldsymbol{\delta_h}$	$\boldsymbol{\delta_t}$
PES	19.6	10.8	9.2	24.19
NMP	18.0	12.3	7.2	22.9
DMAc	16.8	11.5	10.2	22.7
Water	15.5	16	42.3	47.8
Methanol	15.1	12.3	22.3	29.6
Water/Methanol (75/25 V.%)	15.4	15.08	37.3	43.07
Water/Methanol (50/50 V.%)	15.3	14.14	32.26	38.4

Table 3. Mutual diffusivity of various coagulant (c) and solvent (s) systems and the average values (D_m).

System	**Diffusivity coefficient (cm^2.s^{-1})**		
	$\boldsymbol{D_{c-s} \times 10^6}$	$\boldsymbol{D_{s-c} \times 10^6}$	$\boldsymbol{D_m \times 10^6}$
Water-NMP	11.56	7.92	9.74
Water-DMAc	20.89	8.10	14.49
Methanol-DMAc	12.01	6.12	9.06

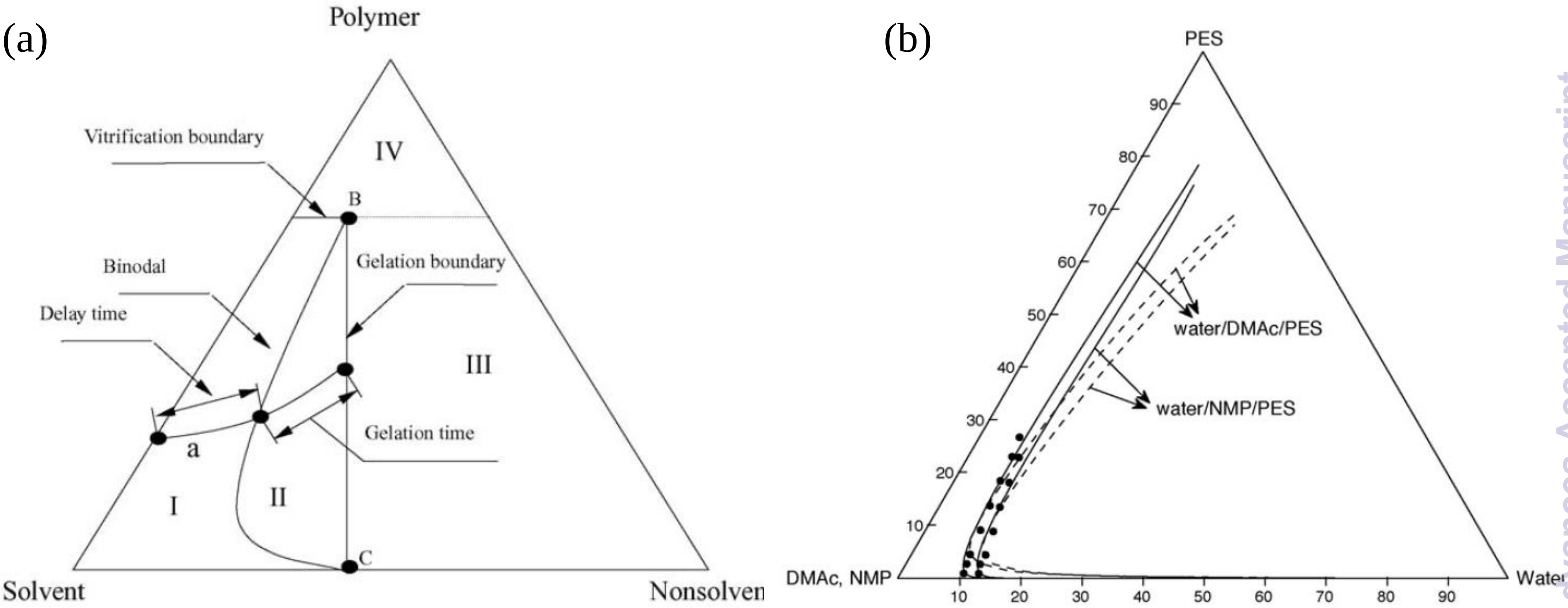

Fig. 6. (a) Schematic representation of a ternary phase diagram [68]; (b) Theoretical binodal (—) and spinodal (– –) curves for water/DMAc/PES and water/NMP/PES systems. Experimental cloud point data (•) verify the theoretical calculations [69].

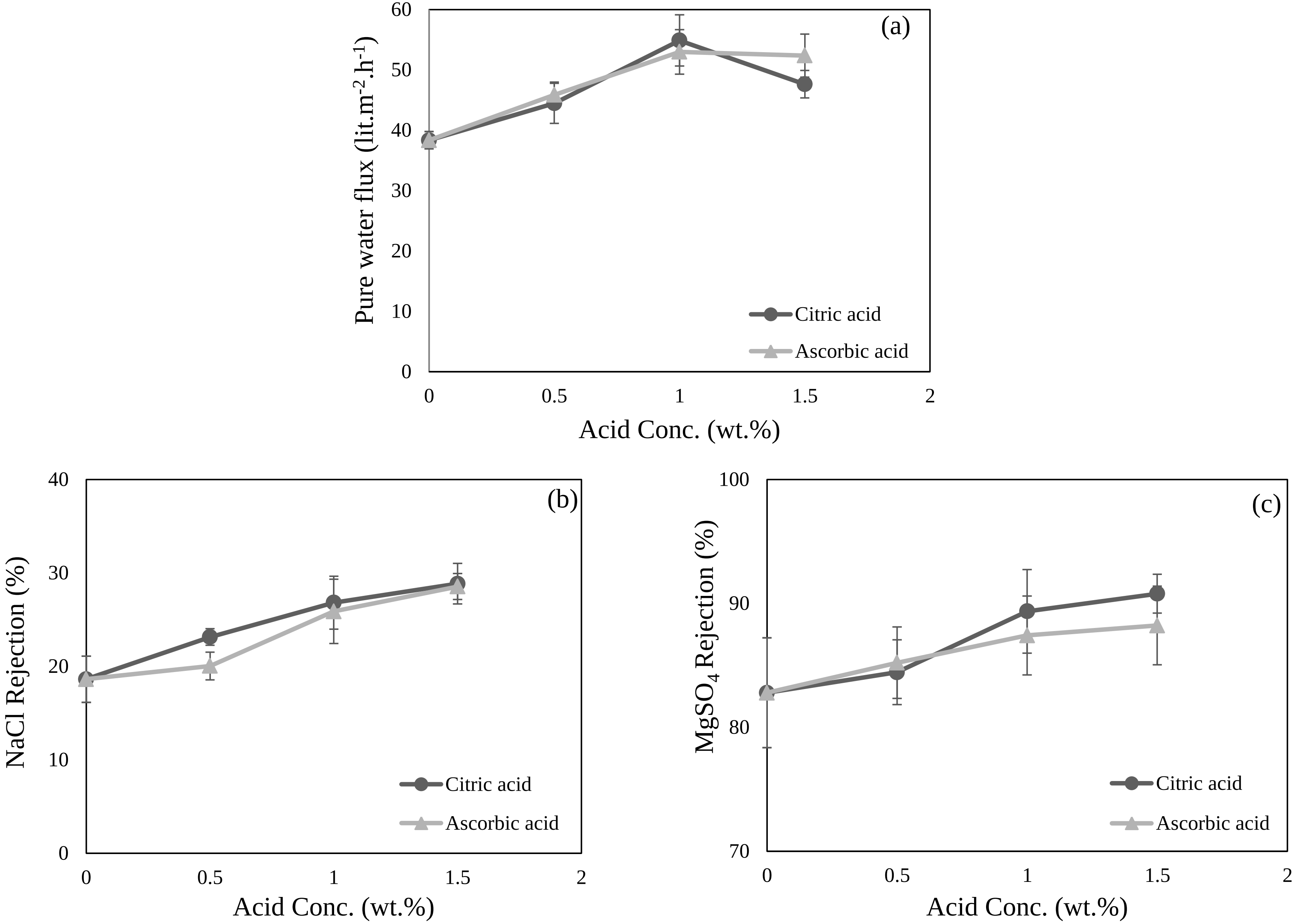

Fig. 7. The effect of type and concentration of organic acids as additives to the dope solutions on (a) pure water flux (b) NaCl rejection (c) $MgSO_4$ rejection of resultant NF membranes.

Table 4. The effect of additives in dope solutions on the structural characteristics of PES NF membranes*.

Additive type	Additive concentration (wt.%)	Solvent concentration (wt.%)	Membrane thickness (μm)	Mean pore size (nm)	Porosity (%)	Contact angle (°)
None	0	76.0	100	4.96	58.9	60.5
Ascorbic Acid	0.5	75.5	93	4.63	67.8	53.1
	1.0	75.0	86	4.51	75.8	43.4
	1.5	74.5	91	4.46	73.8	38.6
Citric Acid	0.5	75.5	96	4.73	66.9	55.7
	1.0	75.0	86	4.44	77.6	48.6
	1.5	74.5	89	4.21	74.7	45.3

* Conditions: Dope solution: 24 wt.% PES in DMAc, Casting temperature: 25±3° C; Relative air humidity: 30±5%; Casting knife gap: 200 μm; Casting shear rate: 23.54 s^{-1}; Solvent evaporation time: 0 min; Coagulating agent: pure water; Coagulation bath temperature: 20±2° C.

Table 5. The effect of coagulating agent on the structural characteristics of PES NF membranes*.

Coagulating agent	**Membrane thickness (µm)**	**Mean pore size (nm)**	**Porosity (%)**	**Contact angle (°)**	**Pure water flux (lit.m^{-2}.h^{-1})**	**NaCl rejection (%)**	**$MgSO_4$ rejection (%)**
Water	100	4.96	58.9	60.5	38.35	18.62	82.78
Water/Methanol (75/25 V.%)	103	4.93	57.2	62.1	35.13	19.17	89.35
Water/Methanol (50/50 V.%)	107	4.68	52.7	65.9	29.15	25.20	91.22

* Conditions: Dope solution: 24 wt.% PES in DMAc, Casting temperature: 25±3° C; Relative air humidity: 30±5%; Casting knife gap: 200 µm; Casting shear rate: 23.54 s^{-1}; Solvent evaporation time: 0 min; Coagulation bath temperature: 20±2° C.

Table 6. The effect of solvent evaporation time and coagulation bath temperature on the structural characteristics of PES NF membranes*.

Solvent evaporation time (min)	**Coagulation bath temperature (° C)**	**Membrane thickness (μm)**	**Mean pore size (nm)**	**Porosity (%)**	**Contact angle (°)**	**Pure water flux (lit.m^{-2}.h^{-1})**	**NaCl rejection (%)**	**$MgSO_4$ rejection (%)**
0	20±2	100	4.96	58.9	60.5	38.35	18.62	82.78
3	20±2	107	4.53	53.7	63.4	26.73	30.65	91.58
0	0±2	111	4.58	52.8	63.3	25.35	31.33	92.25
0	20±2	100	4.96	58.9	60.5	38.35	18.62	82.78
0	50±2	93	5.13	65.2	54.8	52.12	9.25	72.95

* Conditions: Dope solution: 24 wt.% PES in DMAc, Casting temperature: 25±3° C; Relative air humidity: 30±5%; Casting knife gap: 200 μm; Casting shear rate: 23.54 s^{-1}; Coagulating agent: pure water.

Table 7. The effect of casting shear rate and casting knife gap on the structural characteristics of PES NF membranes*.

Casting shear rate (s^{-1})	**Casting knife gap (µm)**	**Membrane thickness (µm)**	**Mean pore size (nm)**	**Porosity (%)**	**Contact angle (°)**	**Pure water flux ($lit.m^{-2}.h^{-1}$)**	**NaCl rejection (%)**	**$MgSO_4$ rejection (%)**
9.23	200	110	5.06	48.3	59.1	25.13	17.12	80.32
23.54	200	100	4.96	58.9	60.5	38.35	18.62	82.78
42.76	200	92	4.54	64.4	60.1	41.32	23.32	89.12
23.54	100	73	5.09	63.6	57.6	56.41	13.54	80.98
23.54	200	100	4.96	58.9	60.5	38.35	18.62	82.78
23.54	300	162	4.59	52.9	65.8	17.87	28.32	90.83

*Conditions: Dope solution: 24 wt.% PES in DMAc, Casting temperature: 25±3° C; Relative air humidity: 30±5%; Solvent evaporation time: 0 min; Coagulating agent: pure water; Coagulation bath temperature: 20±2° C.

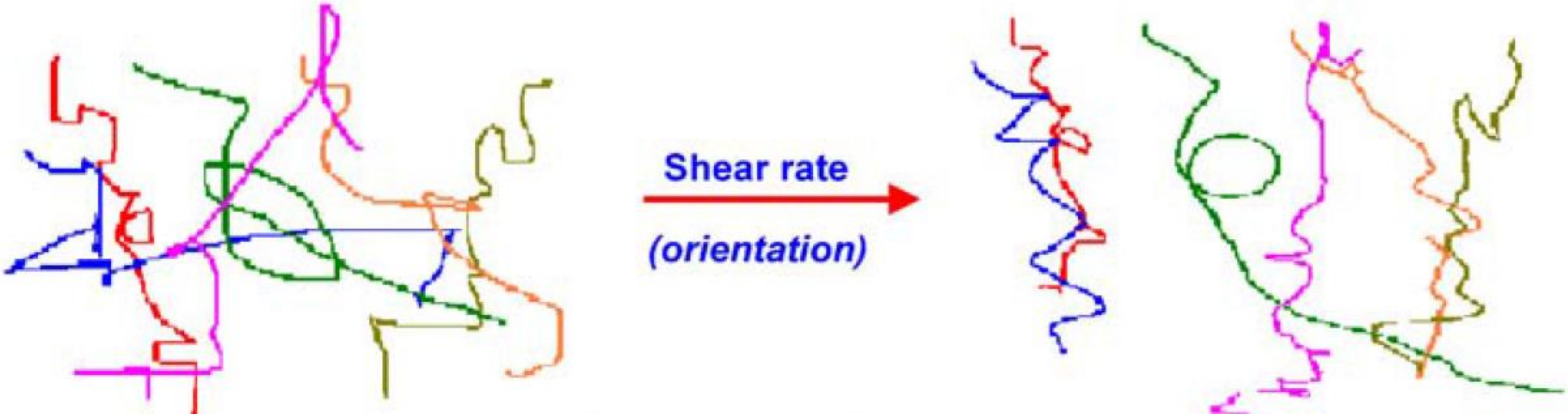

Fig. 8. A hypothetic mechanism for the conformation of polymer chains induced by shear rate [83].

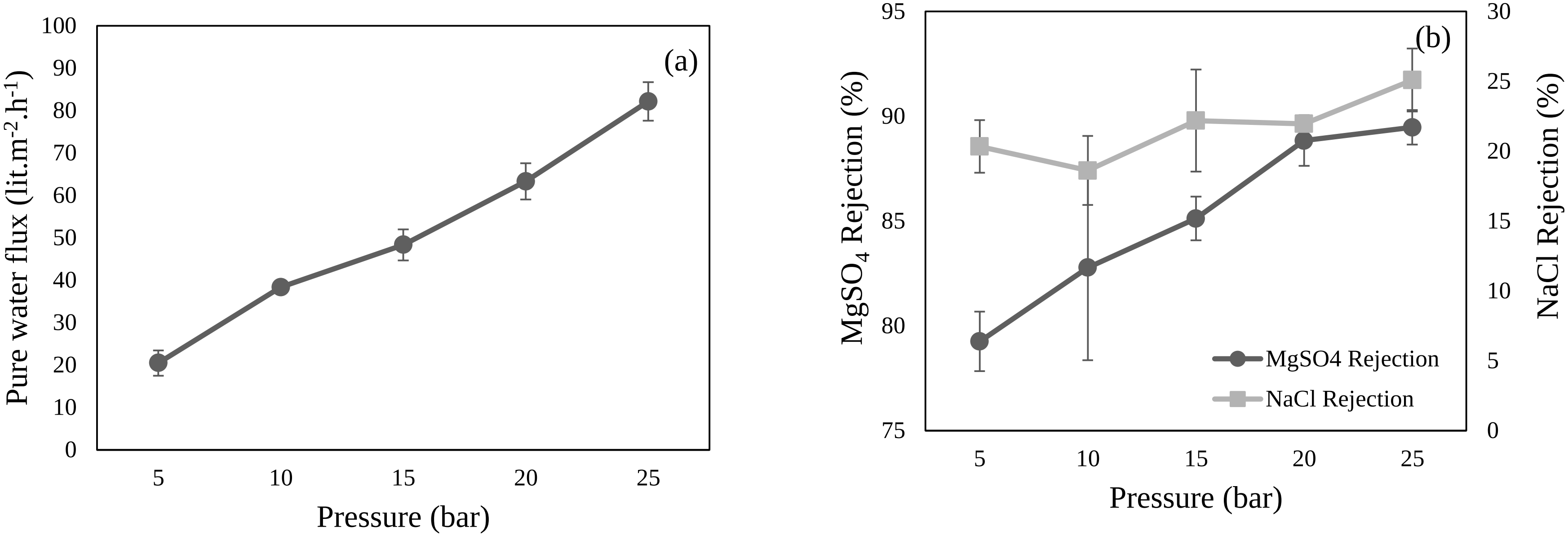

Fig. 9. Effect of feed pressure on (a) pure water flux (b) NaCl and $MgSO_4$ rejection of PES NF membranes. (Conditions: Dope solution: 24 wt.% PES in DMAc, Casting Temperature: 25±3° C; Relative air humidity: 30±5%; Casting knife gap: 200 μm; Casting shear rate: 23.54 s^{-1}; Solvent evaporation time: 0 min; Coagulating agent: pure water; Coagulation bath temperature: 20±2° C; Feed composition: 10,500 ppm NaCl, 1300 ppm $MgSO_4$, pH= 7)

Table 8. The effect of feed pH on water flux and salts rejection of PES NF membranes*.

Feed pH	**Water flux (lit.m^{-2}.h^{-1})**	**NaCl rejection (%)**	**$MgSO_4$ rejection (%)**
5	33.12	12.43	75.47
7	35.21	17.96	81.97
9	37.19	19.65	86.09

* Conditions: Dope solution: 24 wt.% PES in DMAc, Casting temperature: 25±3^{o} C; Relative air humidity: 30±5%; Casting knife gap: 200 μm; Casting shear rate: 23.54 s^{-1}; Solvent evaporation time: 0 min; Coagulating agent: pure water; Coagulation bath temperature: 20±2^{o} C; Feed composition: 10,500 ppm NaCl, 1,300 ppm $MgSO_4$; Testing pressure= 10 bar.

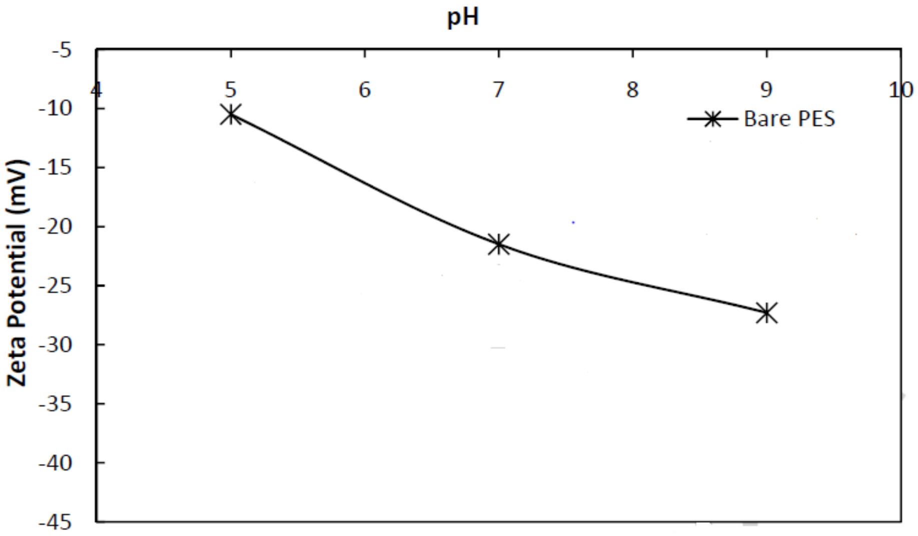

Fig. 10. The zeta potential of the bare membranes as a function of pH [74].

Table 9. Performance comparison for some commercial and non-commercial NF membranes.

Membrane type	**Water flux (lit.m^{-2}.h^{-1})**	**NaCl rejection (%)**	**MgSO$_4$ rejection (%)**	**Operating conditions**	**Ref.**
Polyethersulfone with citric acid as additive	54.88	26.83	89.36	P=10 bar C_{NaCl}=10500 ppm C_{MgSO4}=1300ppm	Present study
Oxidized multiwalled carbon nanotube/ Polyethersulfone nanocomposite	8	20	58	P= 4 bar C=200ppm	[89]
Amine-functionalized multiwalled carbon nanotubes	5.23	20	50	P= 4 bar C=200ppm	[74]
NF90(Commercial)	80	22	99	P=10 bar C=800 ppm	[87]
DS-5 DL (Commercial)	18	1.3	93	P=14 bar	[88]
NE2540-70(Commercial)	NA	7.2	3.56	P=14 bar	[88]